Variational quantum Monte Carlo nonlocal pseudopotential approach to solids: Formulation and application to diamond, graphite, and silicon

S. Fahy
Department of Physics, University of California, Berkeley, Berkeley, California 94720; Materials and Chemical Sciences Division, Lawrence Berkeley Laboratory, Berkeley, California 94720; and AT&T Bell Laboratories, 600 Mountain Avenue, Murray Hill, New Jersey 07974-2070

X. W. Wang and Steven G. Louie
Department of Physics, University of California, Berkeley, Berkeley, California 94720 and Materials and Chemical Sciences Division, Lawrence Berkeley Laboratory, Berkeley, California 94720
(Received 16 March 1990; revised manuscript received 2 July 1990)

A new method of calculating total energies of solids and atoms using nonlocal pseudopotentials in conjunction with the variational quantum Monte Carlo approach is presented in detail. The many-electron wave function is of the form of a Jastrow exponential factor multiplying a Slater determinant. By using pseudopotentials, the large fluctuations of the energies in the core region of the atoms which occur in quantum Monte Carlo all-electron calculations are avoided. The method is applied to calculate the binding energy and structural properties of diamond, graphite, and silicon. The results are in excellent agreement with experiment. Excellent results are also obtained for the electron affinities and ionization potentials of the carbon and silicon atoms.

I. INTRODUCTION

The variational Monte Carlo method, as applied to quantum-mechanical many-body problems, was pioneered by McMillan[1] to study liquid ^{4}He and first applied to fermion problems by Ceperley, Chester, and Kalos.[2] More recently, the Green's-function quantum Monte Carlo approach to the many-electron problem has been applied very successfully to the electron gas,[3] to light molecules,[4] and solid hydrogen.[5] However, a straightforward application of the method to real materials containing heavier atoms has been severely hampered by the very rapid growth in the required computation time with increasing atomic number.[6,7] This growth is caused primarily by the fluctuations in the energies of electrons in the core region. The motivation to overcome this restriction on quantum many-body calculations is high, especially for strongly correlated electronic systems with d and f electrons that are of major current interest and importance. Even in condensed-matter systems where the electronic structure can be said to be reasonably well understood, the standard approach of Hohenberg-Kohn-Sham local-density-functional theory[8] (LDA) has consistently failed to give accurate binding energies[9] although other structural properties may be in good agreement with experiment.

A natural scheme for solving (or at least avoiding) the problems associated with Monte Carlo calculations for the heavier elements is to factor out in some manner the relatively inert core electrons, leaving only the chemically active valence electrons to be treated in the Monte Carlo simulation. This idea of treating the valence behavior only of solids has traditionally been implemented in single-particle theories (e.g., in local-density-functional theory) by the pseudopotential or effective-core-potential approach.[10–13] Using pseudopotentials, the effective atomic number is reduced by including the inert core electrons with the nucleus and treating the interaction of the valence electrons with the core and nucleus combined via an effective potential. The "atomic charge" associated with the pseudopotential is approximately that of the nucleus plus the core electrons, rather than that of the nucleus alone. Thus, in the case of silicon, for example, we reduce the effective "atomic charge" for the system from 14 to 4.

However, in the standard pseudopotential approach, the price paid for this removal of the core electrons from the problem is that the resulting effective potential is angular-momentum dependent.[10] Angular-momentum dependence has usually been achieved by allowing a pseudopotential which involves angular-momentum projection operators and which is thus nonlocal in the angular coordinates. Such a nonlocal potential poses severe problems for the Green's-function Monte Carlo approach and substantial effort has been made to try to circumvent this nonlocality in various ways in the Green's-function quantum Monte Carlo (QMC) method.[7,14–17] We have chosen to accept a nonlocal pseudopotential of the standard form while remaining within the conceptually and computationally simpler variational Monte Carlo approach, where, as we shall see, the nonlocality of the pseudopotential poses less of a problem. As in all variational methods, the applicability of this approach hinges largely on one's ability to employ trial wave functions sufficiently accurate for the level required in estimating the energy

 ©1990 The American Physical Society

(or other quantities) associated with the ground state of the many-body system. As we shall see, we can achieve an accuracy in calculating the energy of carbon- and silicon-based systems, which is substantially better than that achieved by Hohenberg-Kohn density-functional theory within the Kohn-Sham local-density approximation, and very close to that obtained in a Green's-function Monte Carlo calculation.

Through the use of nonlocal pseudopotentials, the present method[18] of performing variational quantum Monte Carlo (QMC) calculations for solids and atoms extends the range of practical applicability of the QMC method for many-fermion systems to real solid-state systems involving heavier ($Z > 2$) elements. The approach has been used to calculate the correlation energy and structural parameters of diamond and silicon and the cohesive energy of graphite. The lattice constants for both diamond and silicon are within one percent of the experimental value. The calculated cohesive energy is 7.45 ± 0.07 eV/atom for diamond, as compared to the experimental value of 7.37 eV/atom,[19] and 7.40 ± 0.08 eV/atom for graphite, compared to 7.40 eV/atom from experiment.[19] This result is thus in significantly better agreement with experiment than the values of 8.63 eV/atom and 8.64 eV/atom for the cohesive energies of diamond and graphite, respectively, obtained using the Hohenberg-Kohn-Sham local-density-functional (LDA) formalism. Typically, LDA binding energies are too large by 15–20%. The LDA gives a cohesive energy for silicon too large by 0.4–0.6 eV/atom, while the present calculation gives a result of 4.88 ± 0.07 eV/atom, in agreement with experiment. However, the comparison with experiment for silicon is not nearly as clean as in the case of diamond and graphite, where the cohesive energy is very-well-determined experimentally;[19] the experimental results[20–25] for the cohesive energy of silicon show a scatter over a range of values from 4.62 to 4.97 eV/atom. The atomic ionization energies and electron affinities for both carbon and silicon are in very good agreement with experiment.[26] Overall, the results indicate that the method can obtain 90–95% of the valence-electron correlation energies in both atomic and solid-state systems.

The rest of the paper is organized as follows. In Sec. II we will review the basic ideas behind the variational Monte Carlo method in general, and, in particular, its application to fermion systems. We discuss in detail the specific form of the correlated wave function used in the present approach in Sec. III. Section IV contains a discussion of the many-body Hamiltonian within a nonlocal pseudopotential approach, along with a detailed outline of its evaluation in conjunction with the correlated wave function. The results of the approach as applied to carbon- and silicon-based systems are given in Sec. V, and the main conclusions of this study are in Sec. VI. In Appendix A, we present some details of the evaluation of the one-body term in the Jastrow factor. Appendix B discusses unbiased sampling of the energy, and Appendices C and D give some details of the statistical evaluation of spherical integrals necessary for the calculation of the nonlocal potential energy.

II. THE VARIATIONAL MONTE CARLO METHOD

The spirit of the variational Monte Carlo approach we will describe in this section is the same as that of all variational estimates for the energies of quantum-mechanical systems.[27] We choose an explicit parametrized form of trial wave function and evaluate the expectation value of the exact Hamiltonian for this wave function. The parameters in the wave function are varied to minimize this expectation value, which then provides an upper bound on the ground-state energy of the system. If we choose the form of the trial wave function with sufficient insight and ingenuity, we hope to obtain not only an upper bound on the ground-state energy, but an accurate estimate of its value.

Since we deal explicitly with the many-body wave functions and Hamiltonian, for a system with N particles, finding this expectation value involves doing a $3N$-dimensional integral,

$$E = \int \Psi^*(\mathbf{r}_1, \ldots, \mathbf{r}_N) H \Psi(\mathbf{r}_1, \ldots, \mathbf{r}_N) d\mathbf{r}_1 \cdots d\mathbf{r}_N \ , \quad (1)$$

where Ψ is a normalized many-body wave function. The form of the wave function usually forbids an analytic evaluation of the integral, and the very large dimension ($3N$) of the configuration space renders impossible the usual fixed-grid techniques of numerical integration. A standard approach to such multidimensional integration is the Monte Carlo method.[28] In the Metropolis algorithm,[29] the integral of a function is calculated by evaluating its average over the points of a random walk through the configuration space of the system:

$$\int f(R)\, d\mu(R) \simeq \langle f \rangle \equiv \frac{1}{n} \sum_{i=1}^{n} f(R_i) W_i \ , \quad (2)$$

where μ is the appropriate measure or probability distribution for the problem, n is the number of steps in the walk, R_i are the points in configuration visited by the walk, and W_i are weighting factors assigned to these points in the evaluation of the integral. The weighting factors depend on μ and the relative probability with which a walk on average visits the points R_i (see below). In this way a statistical estimate of the required multidimensional integral is obtained. For sufficiently long walks, the average $\langle f \rangle$ over the walk has a normal (Gaussian) distribution with an average value equal to the true value of the integral and a standard deviation equal to some constant divided by the square root of the number of steps $\sqrt{n}$ in the walk.[30]

The random walk through the configuration space of the system does not proceed so as to sample all points with equal relative weight. A crucial ingredient[29] in the efficiency of the walk is the idea of "importance sampling," which means, roughly, that points which contribute more to the integral in question (and in that sense are more important) are sampled more often than points which contribute little. More precisely, the random walk is governed so that a point R in the $3N$-dimensional configuration space is visited during the walk with a probability distribution $P(R)$. The role of importance sampling is to reduce drastically the variance of the

Monte Carlo estimator of the integral for a given length of the random walk. Usually, in Monte Carlo integrations of the type we are discussing, there is a "natural" probability distribution or measure with respect to which all quantities are integrated. For example, in classical statistical mechanics,[29] to find the average of any quantity Q over the canonical ensemble we take

$$\langle Q \rangle = \frac{1}{Z} \int Q(R) \exp[-\beta E(R)] dR \ , \tag{3}$$

where Z is the partition function. Here the probability measure is specified by

$$d\mu(R) \equiv \frac{1}{Z} \exp[-\beta E(R)] dR \ . \tag{4}$$

In quantum-mechanical problems,[1] the probability measure is determined by the square modulus of the normalized wave function:

$$d\mu(R) \equiv |\Psi(R)|^2 dR \ . \tag{5}$$

If the random walk proceeds so as to sample the points in configuration space with the probability distribution of the natural measure of the problem, then the weights W_i in Eq. (2) are equal to unity.[1] In the more general situation, $W(R) = d\mu(R)/[P(R)dR]$.

In order to achieve the probability distribution $P(R)$ asymptotically for points in the random walk, the configuration of the particles at each step of the walk is generated from the previous configuration by changing the coordinates of one particle at random in the following way: Choose a vector $\Delta \mathbf{r}$ so that each of its components has a uniform distribution in the interval $[-S, S]$, where S is a fixed "step length" chosen in a manner described below. Then we decide whether to accept or reject the move

$$\mathbf{r}_i \rightarrow \mathbf{r}_i + \Delta \mathbf{r} = \mathbf{r}_i' \ . \tag{6}$$

If $\eta = P(R')/P(R)$ is greater than 1, we always accept the move and make the trial configuration R' the next configuration on the random walk [$P(R) = |\Psi(R)|^2$ in the present case]. If η is less than 1, we accept the move with probability η. If the move is rejected, we make the old configuration R the next configuration on the random walk. The coordinates of each particle in turn are changed in this manner, starting with the first particle, and returning to the first particle when the last one has been updated.

When the walk proceeds for long enough (typically several hundred steps per particle in the present applications, where the number of particles is of the order of one hundred) the relative probability of visiting the configurations R and R' is $P(R)/P(R')$. To see this,[1,28] consider many such walks proceeding independently at once. The distribution of walks will reach equilibrium when the number of points moving from R to R' equals the number going in the opposite direction, from R' to R. Suppose R can be reached from R' in one step. Let $P(R \rightarrow R')$ be the probability of accepting a move from R to R' and $N(R)$ be the density of points at R. Since the probability density of choosing R' as a *trial* configuration from R is the same as that of choosing R from R', then at equilibrium

$$N(R)P(R \rightarrow R') = N(R')P(R' \rightarrow R) \ . \tag{7}$$

This equilibrium density, $N(R)$, will be the correct distribution if

$$\frac{P(R)}{P(R')} = \frac{N(R)}{N(R')} \ . \tag{8}$$

This gives us the condition on the rule for accepting moves:

$$\frac{P(R' \rightarrow R)}{P(R \rightarrow R')} = \frac{P(R)}{P(R')} \ . \tag{9}$$

There are many ways of satisfying this relation. A standard and simple one is the method we use, where

$$P(R \rightarrow R') = \min \left\{ 1, \frac{P(R')}{P(R)} \right\} . \tag{10}$$

If the relation (9) holds for all points which can be reached by one step from R, it is easy to see that it must also hold for all points R' which can be reached in a finite number of steps from R. The walk is said to be ergodic if any two points in the configuration space can be reached from each other by a finite number of steps of the walk. We will assume that the walks are ergodic for all practical purposes and sample all of the configuration space effectively. We note that the estimation of expectation values of variables with respect to $P(R)$ given in Eq. (2) automatically normalizes the distribution $P(R)$ when the W_i are equal to unity. In the more general case, the distribution can be normalized by dividing by $\sum_1^n W_i$ instead of by n, as is done in Eq. (2).

In the practical calculation of averages over the random walk we do not use the simple sum in Eq. (2) over the points of the walk which are accepted. Rather, following Ref. 2, we use an equivalent form which incorporates information about trial moves which are eventually rejected. If R_i' is the *trial* position at the ith move in the random walk, then the average over the walk is taken as

$$\langle f \rangle \equiv \frac{1}{n} \sum_{i=1}^{n} \{ [1 - P(R_i \rightarrow R_i')] f(R_i) + P(R_i \rightarrow R_i') f(R_i') \} \ . \tag{11}$$

This estimator has the same average as the simple sum over accepted configurations of the walk but usually has a smaller variance, since it reduces the fluctuations caused by acceptance of unlikely configurations.

III. THE MANY-BODY WAVE FUNCTION

For bosons the many-body wave function is a symmetric function of the positions of the particles. In studying the ground state of liquid He by the variational Monte Carlo method,[1] McMillan used a form of the many-body wave function given by the Jastrow function[31–35]

$$\Psi(R)=\Psi(\mathbf{r}_1,\ldots,\mathbf{r}_N)=\exp\left[-\sum_{i\le i<j\le N}u(r_{ij})\right], \quad (12)$$

where $u(r)$ is a function of r, chosen variationally to minimize the energy of the state. The function u is chosen to enhance the probability of pairs of He atoms being separated by a distance where their interaction energy is a minimum. In this way, although a price is paid in increased kinetic energy of confinement, the total energy is reduced.

In the present work, we will be concerned not with boson problems, but exclusively with fermion problems where the many-body wave function is antisymmetric.[2] The nuclei in the solid will be treated simply as sources of an external potential and will be held fixed at the ideal lattice positions. Only the many-body wave function of the valence electrons will be considered. In the Hartree-Fock approximation, the simplest antisymmetric function is used, viz., a single Slater determinant. One of the advantages of this approximation is that the variational problem can be expressed in terms of a set of self-consistent single-particle equations, the Hartree-Fock equations, which can be solved directly. However, apart from the antisymmetric form of the wave function, there is no correlation between the electrons in this approximation. The introduction of correlation should keep the electrons from coming close together, particularly those of opposite spin, which are not correlated in any way in the Hartree-Fock approximation, thus reducing the Coulomb interaction energy.

In analogy with the boson problem, a convenient and physically appealing way of introducing correlation is to multiply the Slater determinant by a Jastrow factor,[35] as in Eq. (12). This form of correlated wave function has been used as the starting point for many methods in the past.[2,35–37] Our approach follows the work of Ceperley, Chester, and Kalos[2] on uniform fermion systems. When $u(r)$ is a positive and decreasing function of r, the probability of two electrons coming close together is reduced and the repulsive electron-electron interaction energy is reduced. As in the boson problem, the kinetic energy and other terms in the energy are increased by the introduction of the Jastrow factor and so $u(r)$ is chosen variationally to obtain the optimum energy. This many-body wave function can be conveniently sampled using the variational quantum Monte Carlo approach, although in practice its optimal form cannot be determined exactly via a self-consistent single-particle theory, as can the Hartree-Fock wave function.

A further complication arises in the inhomogeneous systems we will study, over and above that of Fermi statistics. In principle, the two-body term in the Jastrow factor is no longer a function $u(r_{ij})$ of the distance r_{ij} between electrons i and j, but rather a function $u(\mathbf{r}_i,\mathbf{r}_j)$ of each coordinate separately. [Formally, the solution of the Euler-Lagrange equation for arbitrary $u(\mathbf{r}_i,\mathbf{r}_j)$ may be stated as follows:[38] for the optimal u, the energy of the system when particle 1 is constrained at position $\mathbf{r}_1$ and particle 2 at $\mathbf{r}_2$ is independent of the values of $\mathbf{r}_1$ and $\mathbf{r}_2$.] An even more serious consideration is that the presence of the Jastrow factor alters the single-particle density obtained from the Slater determinant alone in an inhomogeneous system. Even neglecting three- and more-body terms in the Jastrow factor, which can be envisaged but might be guessed on physical grounds to be relatively unimportant in homogeneous and inhomogeneous systems alike, the interplay between the one- and two-body terms in the Jastrow factor and the single-particle wave functions of the Slater determinant in minimizing the energy is complex and has not been solved exactly. The Fermi hypernetted-chain approach allows one to develop a self-consistent approach to this problem,[37] but only within the approximations of that method for the energy as a functional of the Jastrow factor and Slater determinant.

In practical application of the variational Monte Carlo approach, we will be forced to make restrictions on the forms of the one- and two-body terms we use in the Jastrow factor, although the energy will be evaluated exactly for any given form, so that the results remain variational. Perhaps a central result of the present work is that a surprisingly simple form of the Jastrow factor can give excellent results for the energies of the systems we have considered. In particular, the many-body wave function we use is of the form

$$\Psi(R)=\Psi_J(R)d^{\uparrow}(R)d^{\downarrow}(R)\ . \quad (13)$$

The Jastrow factor Ψ_J is of the form

$$\Psi_J(R)=\exp\left[\sum_{(s,i)=(\uparrow,1)}^{(\downarrow,N)}\chi_s(\mathbf{r}_i^s)-\sum_{(\uparrow,1)\le(s,i)<(s',j)}^{(\downarrow,N)}u_{ss'}(r_{ij})\right]. \quad (14)$$

The two-body term $u(r_{ij})$ is assumed to depend only on the distance r_{ij} between the particles and on their relative spin. The effectiveness of this approximation can only be assessed after the fact by the results obtained from it. The results we present below clearly demonstrate its adequacy at least in the *sp* electron systems we have studied, where 90–95 % of the correlation energies are obtained. The term d^s is the Slater determinant for electrons with spin s. The one-body term $\chi(\mathbf{r}_i)$ in the Jastrow factor could be formally incorporated into the Slater determinant by multiplying each single-particle orbital by $\exp[\chi(\mathbf{r})]$. However, it is convenient in the calculation to keep it in the Jastrow factor, using it to vary the single-particle density to minimize the energy.

The two-body function $u(r_{ij})$ in the Jastrow factor is chosen for the solid to be of the standard form[39]

$$u(r)=A(1-e^{-r/F})/r\ , \quad (15)$$

where A and F are variational parameters. This function has the general behavior one intuitively expects: u is large and positive for $r=0$ and decreases to zero as $r\to\infty$. From the Euler-Lagrange equation for u mentioned above, it follows[38] that, as two electrons approach one another, the divergence of the Coulomb interaction between them must be accompanied by an equal and opposite divergence of the kinetic energy. This yields the following condition (for three-dimensional systems) on

the derivative of u (in atomic units) at $r=0$:

$$\left.\frac{du}{dr}\right|_{r=0} = \begin{cases} -\frac{1}{2} & \text{for opposite spin} \\ -\frac{1}{4} & \text{for parallel spin} . \end{cases} \quad (16)$$

This "cusp" condition holds in both the atom and the solid and is independent of electron density. A relative-spin-dependent value of F is used to satisfy this condition. As discussed in previous work on the uniform electron gas,[39,40] the behavior of u as $r\to\infty$ is dominated by the zero-point motion of the plasmons in the solid, leading to a $1/r$ dependence with a coefficient equal to $e^2/\hbar\omega_p$. Although the solids we are studying are insulators, this condition should not be expected to change much there, since the plasma frequency is substantially larger than the band gap.[41] Indeed, the experimentally measured plasma frequency in diamond and silicon is virtually identical to that obtained from the uniform electron gas with a density equal to the average valence charge density for the crystal.

We have varied the value of A while maintaining the cusp condition at $r=0$ for both parallel and opposite spin electrons and have found its optimal value in diamond to be just that obtained from consideration of the zero-point plasmon motion. In graphite the experimental plasmon spectrum is no longer dominated by a single peak[41] at the ideal value calculated from the average valence charge density. However, even in this case we find the variationally obtained optimal value of A to be only 5% larger than the ideal value for a uniform electron gas at the same average density. The difference in energy due to this difference in A is negligible. Of course, there is no obvious reason why the intermediate-range behavior u should be ideal for a particular choice of A and F, even if the short- and long-range behavior is correct. With this in mind, we have examined the effect on the energy in diamond of adding to u an intermediate range term of the form $C\exp[-(r/r_s)^2]$, where $4\pi r_s^3/3$ equals the average crystal electron density and C is a variational parameter. This term leaves the slope at the origin and the long-range behavior of u unchanged. We find the optimal value of C to be very close to zero and the gain in energy from the introduction of this term to be negligible.

For atoms, we have used both the form of $u(r)$ for the solid and the form

$$u(r)=-ar/(1+br) , \quad (17)$$

where a is fixed by the cusp condition at $r=0$ for opposite and parallel spin and $\beta=\sqrt{a/b}$ is a single variational parameter. The energies obtained from the two forms agree within statistical noise of 0.04 eV per atom.

The one-body term $\chi(\mathbf{r})$ in the Jastrow factor allows a variational adjustment of the electron charge density in the presence of the two-body term $u(r_{ij})$. Its importance has previously been observed in the context of hypernetted-chain calculations for inhomogeneous systems. The two-body term tends to make the charge density more uniform than that obtained from the Slater determinant alone, reducing charge density in higher density regions and increasing that in lower density regions. This is an unavoidable effect of the introduction of the two-body term in an inhomogeneous system, although the intuitive motivation for its introduction is to change the pair-correlation function, *not* the single-particle density, which may be already assumed to be quite well optimized by the solution of the mean-field single-particle (Hartree-Fock or LDA) problem. In the calculations discussed here, we either simply set

$$\chi(\mathbf{r})=\tfrac{1}{2}\alpha\ln[\rho_{\chi,\,u=0}(\mathbf{r})/\rho_{\chi=0}(\mathbf{r})] , \quad (18)$$

where $\rho(\mathbf{r})$ is the charge density and α is a variational parameter, or in the case where the LDA charge density (i.e., that from the Slater determinant of LDA orbitals alone) is significantly different from the QMC charge density for $\chi=0$ and $u\neq 0$, as is the case in the atoms and in graphite, we iteratively find $\chi(\mathbf{r})$ by setting

$$\chi(\mathbf{r})=\sum_i \chi_i(\mathbf{r}) , \quad (19)$$

where χ_1 is given by the previous expression [Eq. (18)] and

$$\chi_{i+1}(\mathbf{r})=\tfrac{1}{2}\alpha\ln[\rho_{\chi,\,u=0}(\mathbf{r})/\rho_{\chi_i}(\mathbf{r})] . \quad (20)$$

In practice, as discussed in detail in Appendix A, we calculate the Fourier components of χ, so that the χ which is finally used in the many-body wave function is the form

$$\chi(\mathbf{r})=\sum_{\mathbf{G}} \chi(\mathbf{G})\exp(i\mathbf{G}\cdot\mathbf{r}) . \quad (21)$$

This form allows for rapid calculation of χ and its derivatives during the random walk.

The Slater determinant d^s for electrons with spin s is the determinant of the Slater matrix, $\underline{D}$, where

$$D_{ji}=\phi_j(\mathbf{r}_i^s) . \quad (22)$$

Here the ϕ_j are a set of N single-particle wave functions. For simulation of infinite systems, they satisfy periodic boundary conditions on the simulation region. (For simulations of crystals, the simulation region consists of some integral number of crystal unit cells.) In practice, a suitable choice of such single-particle wave functions is the set of wave functions obtained from the corresponding local-density-functional calculation.[8] In the systems discussed here, the LDA wave functions are essentially indistinguishable from the Hartree-Fock wave functions.[36,42] Thus it appears that any reasonable mean-field approximation for the single-particle problem gives the same wave functions. This is not universally true, and in systems where the LDA and Hartree-Fock wave functions differ significantly, the use of either set is more suspect. In all cases it is not possible to rigorously justify the use of either LDA or Hartree-Fock wave functions in the Slater determinant when a Jastrow factor is present. However, important atomic (electron-ion) information is embodied in these wave functions which would otherwise be difficult to reproduce with a simple parametrization of the single-particle wave functions. This is clearly revealed by the fact that the energy of the many-body wave function calculated in the quantum Monte Carlo method follows the same convergence with respect to the number of basis functions used to solve for the LDA wave func-

tions as does the LDA energy itself; e.g., a lowering of 0.2 eV per atom in the LDA total energy of diamond due to the inclusion of d states in the linear combination of atomic orbitals (LCAO) basis is matched by the same reduction in the QMC energy when these more accurate LDA wave functions are used in the Slater determinant. Ultimately, one must always appeal to the variational nature of the QMC calculation and incorporate as much intuition about the chemical nature of the system into the many-body wave function as possible to minimize its energy. In this context, it would be most interesting to have available chemically accurate wave functions for both atoms and solid-state systems generated from the Fermi-hypernetted-chain approximation in the presence of a Jastrow factor.

The value of the Slater determinant at each move of the Monte Carlo walk can be calculated as follows.[2] Note that changing the position of one of the particles changes just one row of the Slater matrix. Also recall that the inverse of the transpose of a matrix is equal to the matrix of cofactors divided by the determinant. Moreover, the cofactor of an element (i,j) in a matrix does not depend on the matrix elements in the ith row or the jth column. Using these facts, it follows that if we change the ith row of the matrix to get a new matrix, the ratio of the new to old determinants is given by

$$\frac{d_{\text{new}}}{d_{\text{old}}}=q_i=\sum_{j=1}^{N}\tilde{D}_{ji,\text{old}}D_{ji,\text{new}}\ , \tag{23}$$

where $\underline{\tilde{D}}$ is the inverse of the transpose of the matrix $\underline{D}$, i.e., $\underline{\tilde{D}}=(\underline{D}^t)^{-1}$. Thus in the case of the Slater determinant for spin s, the ratio is

$$q_i^s=\sum_{j=1}^{N}\tilde{D}^{\,s}_{ji,\text{old}}\phi_j(\mathbf{r}^s_{i,\text{new}})\ . \tag{24}$$

The ratio of the Jastrow factors for the old and new configurations is

$$\frac{\Psi_J(R_{\text{new}})}{\Psi_J(R_{\text{old}})}=\exp\left[\sum_{\substack{(s',j)=(\uparrow,1)\\(s',j)\neq(s,i)}}^{(\downarrow,N)}[u(|\mathbf{r}_j^{s'}-\mathbf{r}^s_{i,\text{old}}|)-u(|\mathbf{r}_j^{s'}-\mathbf{r}^s_{i,\text{new}}|)]-\chi(\mathbf{r}^s_{i,\text{old}})+\chi(\mathbf{r}^s_{i,\text{new}})\right]\ . \tag{25}$$

In keeping with the periodic boundary conditions in the simulation of infinite systems, we sum (s',j) over all images of the particles in the simulation region.

From Eqs. (24) and (25) we see that calculating the ratio of the new to old wave functions takes order N arithmetic operations. If the move is accepted the matrix $\underline{\tilde{D}}$ must be updated, an operation which requires order N^2 operations. The new matrix $\underline{\tilde{D}}$ can be calculated from the old by the substitutions

$$\tilde{D}^{\,s}_{jk}=\begin{cases}\tilde{D}^{\,s}_{jk}/q^s, & k=i\\ \tilde{D}^{\,s}_{jk}-\dfrac{\tilde{D}^{\,s}_{ji}}{q^s}\left[\displaystyle\sum_{l=1}^{N}\tilde{D}^{\,s}_{lk}\phi_l(\mathbf{r}_i^s)\right], & k\neq i\ .\end{cases} \tag{26}$$

Thus we see that the special properties of the Slater determinant allow efficient evaluation of the ratio of the old to new wave functions along the Monte Carlo random walk, a very important point in the practical implementation of the method.

Although trivial in principle, the evaluation of the single-particle wave functions in the Slater determinant is a matter of considerable computational importance and difficulty. In order to avoid excessive computation time in their evaluation, they must be expressed in a reasonably compact representation suitable for rapid numerical calculation. On the other hand, the representation must give accurate numerical values if useful information is to be obtained from the Monte Carlo simulation. In crystals, the single-particle orbitals may be written in Bloch form, $\phi_{n\mathbf{k}}(\mathbf{r})=\exp(i\mathbf{k}\cdot\mathbf{r})u_{n\mathbf{k}}(\mathbf{r})$, where u is periodic. We adopt a composite of LCAO (Ref. 43) and plane-wave[44] representations for ϕ. The method is in some ways reminiscent of the Ewald summation technique[45] and is similar to the mixed-basis[46] approach to single-particle electronic-structure calculations. Our density-functional calculations for diamond and graphite provide the wave functions in the LCAO representation as output. In the evaluation of the wave functions in the Monte Carlo program, we leave the short-range Gaussian orbitals in their original representation and take the plane-wave representation of the long-range orbitals prior to the Monte Carlo calculation. Each single-particle wave function is expressed as a sum of both localized Gaussian orbitals and plane waves. Thus, to evaluate the single-particle wave functions at a particular point, we need to determine the Gaussian orbital sites within a cutoff radius large enough to ensure that the short-range orbitals from sites outside that radius are negligibly small at the point. The Gaussian part can be evaluated directly from the LCAO representation[43] of the LDA wave functions:

$$u_{\text{loc}}(\mathbf{r})\equiv\sum_{\substack{\mathbf{R},\alpha,l,m\\(|\mathbf{r}-\mathbf{R}|<R_{\text{cut}})}}C_{\alpha lm}f_{\alpha lm}(\mathbf{r}-\mathbf{R})\exp[i\mathbf{k}\cdot(\mathbf{R}-\mathbf{r})]\ , \tag{27}$$

where u denotes the periodic part of the wave function, $f_{\alpha lm}$ are the LCAO basis functions, $C_{\alpha lm}$ are the LCAO expansion coefficients of the wave function, $\mathbf{k}$ is the $\mathbf{k}$ point to which the wave function belongs, and R_{cut} is the appropriately chosen cutoff radius. The plane-wave part is evaluated directly as a sum of exponentials:

$$u_{\text{PW}}(\mathbf{r})\equiv\sum_{\substack{\mathbf{G}\\(|\mathbf{G}|<G_{\text{cut}})}}C_{\mathbf{G}}\exp(i\mathbf{G}\cdot\mathbf{r})\ , \tag{28}$$

where $\mathbf{G}$ are vectors of the reciprocal lattice with length

less than an appropriate cutoff, $G_{\rm cut}$. Several hundred plane waves can be used in practice in this summation since the exponentials and dot products can be evaluated very efficiently on vector processors.

Considerable care must be exercised to ensure that the calculation of the kinetic energy from the representation of the single-particle wave functions is consistent with the calculated values of the wave functions. Surprisingly small discontinuities in the wave function due to too small a cutoff radius for the inclusion of neighboring sites can cause substantial errors in the total energy obtained. Internal consistency in the evaluation of the kinetic energies and values of the wave functions is even more important than the accuracy of the representation of the LDA single-particle wave functions. For crystalline silicon, a plane-wave LDA calculation was performed to calculate the single-particle wave functions in advance and a pure plane-wave representation was used to evaluate the single-particle wave functions in the QMC calculation for the results reported here. Some calculations were also repeated in the mixed representation to cross check results. Some of the diamond results were also cross checked by transforming *all* the Gaussian basis orbitals into plane waves and repeating the calculations in the resulting pure plane-wave representation. In the atoms, the wave functions are tabulated on a very fine radial grid of several thousand points, and calculated by interpolation.

IV. THE HAMILTONIAN

In this section we describe the many-body Hamiltonian used for infinite crystals within the pseudopotential[11] formalism. The essential ingredients in the Hamiltonian are an external potential (due to the ions in the crystal), the kinetic energy of the valence electrons, and the Coulomb interaction between the valence electrons.

The external potential has two parts to it: a local part and a nonlocal part. The local part is diagonal in the coordinate representation of the electrons and can be written as

$$E_{\rm loc}=\sum_{\mathbf{R},(s,i)} V_{\rm ion}(\mathbf{r}_i^s-\mathbf{R}) , \tag{29}$$

where the $\mathbf{R}$ are the positions of the ions in the crystal and the $V_{\rm ion}(\mathbf{r})$ are the local pseudopotentials of the ions. The nonlocal part is much more complicated and we leave writing its precise form until Sec. IV B. We merely note at this stage that it is not diagonal in the coordinate representation of the electrons and involves the evaluation of the many-body wave function for positions of the ith particle on a sphere about each atom.

The kinetic energy has the usual form,

$$E_{\rm kinetic}=-\frac{\hbar^2}{2m}\sum_{(s,i)}\nabla^2_{(s,i)} , \tag{30}$$

and the Coulomb interaction between the electrons is given by

$$E_{\rm el\text{-}el}=\tfrac{1}{2}\sum_{(s,i)}\sum_{(s,j')\neq(s,i)}\frac{e^2}{|\mathbf{r}_j^{s'}-\mathbf{r}_i^s|} , \tag{31}$$

where, in keeping with the periodic boundary conditions of the simulation region, the sum over (s',j) is taken over all images of the particle (s',j) in the simulation region.

In this Monte Carlo calculation we do not in fact sample the *total* energy of the $2N$ particle system at each point of the random walk. Rather, we calculate the energy of the particle being moved at each step of the walk; if particle (s,i) is being moved, we only include the terms involving (s,i) in the above expressions for the total energy. In this way we obtain an unbiased estimator of the energy per particle (defined as the total energy, divided by the number of particles). See Appendix B for further discussion of this point.

A. The local pseudopotential

Here we describe in detail how the local pseudopotential energy is evaluated during the Monte Carlo random walk. The resulting expression is used to calculate the energy of the particle most recently moved in the random-walk process. We leave the description of the more complex problem of the nonlocal pseudopotentials until Sec. IV B. The pseudopotentials we use are those generated by the scheme of Hamann, Schlüter, and Chiang[11] for use in local-density-functional calculations.[8] These smooth ionic potentials tend rapidly to the all-electron electrostatic potential of the nucleus plus core electrons, $-Z_{\rm ion}/r$, beyond a cutoff radius r_c of the order of one atomic unit and give valence eigenvalues (and eigenfunctions outside of r_c) virtually identical to the all-electron density-functional calculations.

A fundamental objection might perhaps be raised to the use of these potentials on the grounds that they are objects derived from density-functional-theory calculations of the atom and should only be used within the context of density-functional theory in the solid. From a purely logical standpoint, this objection is well founded and the use of such pseudopotentials cannot be rigorously justified. Presumably, for systems in which core-valence exchange and correlation play a very important role, this approach could give poor results. However, calculations such as those of Hybertsen and Louie[47] for quasiparticle energies indicate that this is not the case in many insulators, semiconductors, and metals. We expect that the pseudopotentials generated from density-functional theory will give a reasonable description of the core-valence interaction for the variational calculations. Also, since the ground-state properties are determined by differences in total energies, the dominant many-body contributions to these differences would be from changes in the valence-valence electron correlations, and the core-valence effects are expected to cancel out or to play a relatively minor role.

At worst, we can consider these to be model calculations designed to approximate the behavior of the corresponding real system. The validity of the model can then be judged *a posteriori* by the accuracy of the predictions it makes for the properties of the real system. The generation of a one-body pseudopotential rigorously derived from all-electron many-body calculations for use in valence-electron many-body calculations remains an open

problem. Indeed, it is not even clear how such a problem should be formulated in principle or what properties of the all-electron many-body eigenfunctions should be reproduced in the valence-electron many-body eigenfunctions. An appropriate solution to this problem is of great interest.

The LDA local pseudopotential at any point in the crystal is a sum of the potentials of the ions evaluated at that point:

$$V(\mathbf{r})=\sum_{\mathbf{R}_{\rm ion}} V_{\rm ion}(|\mathbf{r}-\mathbf{R}_{\rm ion}|)\ , \tag{32}$$

where $\mathbf{R}_{\rm ion}$ are the positions of the ions and $V_{\rm ion}(r)$ is the (spherically symmetric) potential due to the ion at a distance r. In fact, as it stands, the sum in Eq. (32) does not even converge for the infinite crystal because of the long-range $1/r$ tail of the ionic pseudopotential. However, we implicitly assume that we include the electrostatic potential of a counterbalancing uniform negative background charge equal in density to the average charge density of the ions. [The interaction of the electron at the point $\mathbf{r}$ with this uniform background charge is in turn balanced by an equal and opposite interaction with the positive background introduced in the evaluation of the electron-electron interaction (see below). When these are added we are left only with the true interaction of the electron with the combined electron-ion system.]

Even with the addition of the uniform negative background, the sum in Eq. (32) converges very slowly as a function of the number of nearest neighbors included. A much more satisfactory approach is to divide each ion potential into a $-Z_{\rm ion}/r$ part and a deviation from $-Z_{\rm ion}/r$ behavior. As we mentioned above, this deviation from $-Z_{\rm ion}/r$ has a range of only a few atomic units and can be expressed at any point in the crystal as a sum of contributions from a small number of neighboring ions. The $1/r$ part can be evaluated by the usual Ewald summation technique,[48] in which the sum is divided into a "real-space" part and a "Fourier-space" part, each of which converges rapidly. The terms in the real-space sum converge like $\mathrm{erfc}(-\sqrt{\alpha}r)/r$, where erfc is the complementary error function, and those in Fourier space like $(e^{-G^2/4\alpha})/G^2$. Here α is a parameter which can be varied to optimize the efficiency of the method. (The converged value of the real- plus Fourier-space sums is independent of α.)

Combining the deviation from $-Z_{\rm ion}/r$ behavior with the real-space part of the Ewald sum gives the potential at a point in the crystal as a sum over the positions of the ions plus a sum over reciprocal-lattice vectors:

$$V(\mathbf{r})=\sum_{\substack{R_{\rm ion}\\(|\mathbf{r}-\mathbf{R}_{\rm ion}|<R_{\max})}} V^R_{\rm ion}(|\mathbf{r}-\mathbf{R}_{\rm ion}|) + \sum_{\substack{\mathbf{G}\\(G<G_{\max})}} V^F(G)\,S(\mathbf{G})\exp(i\mathbf{G}\cdot\mathbf{r})\ . \tag{33}$$

Here $R_{\max}$ and $G_{\max}$ are cutoff radii in real and Fourier space, respectively, chosen to give the required accuracy in the value of $V(\mathbf{r})$. The potentials in real and Fourier space are given by

$$V^R_{\rm ion}(r)=V_{\rm ion}(r)+\frac{Z_{\rm ion}}{r}[1-\mathrm{erfc}(\sqrt{\alpha}r)]\ , \tag{34}$$

$$V^F(G)=\begin{cases}\dfrac{4\pi\exp(-G^2/4\alpha)}{G^2 V_{\rm cell}} & \text{for } G\neq 0\\[2ex] -\dfrac{\pi}{V_{\rm cell}\alpha} & \text{for } G=0\ ,\end{cases} \tag{35}$$

where $V_{\rm cell}$ is the volume of the crystal unit cell. Comparable convergence is obtained for the real and Fourier space sums when $\alpha R^2_{\max}=G^2_{\max}/4\alpha$. The structure factors $S(\mathbf{G})$ of the ionic charge are

$$S(\mathbf{G})\equiv\sum_{\mathbf{R}_{\rm ion}\in\text{unit cell}} -Z_{\rm ion}\exp(-i\mathbf{G}\cdot\mathbf{R}_{\rm ion})\ . \tag{36}$$

The real-space potential $V^R_{\rm ion}(r)$ is tabulated on a fine radial mesh and evaluated by interpolation at each step of the random walk. The Fourier-space potential is also calculated in advance.

In the atomic calculations, the local potential is evaluated at the position of the electron by interpolation from values tabulated in advance on a fine uniform radial grid.

B. The nonlocal pseudopotential

We now develop the basic equation for evaluating the contribution to the energy per particle from the nonlocal pseudopotential of the ions within the Monte Carlo scheme for importance sampling of the many-body wave function. The resulting equation is used to calculate the energy of the particle most recently moved in the random-walk process. Some details of the numerical evaluation of the integrals involved in the nonlocal energy are presented in Appendixes C and D.

First we write down that part of the many-body Hamiltonian which arises from the nonlocal pseudopotential of the ions. This must be a simple (linear) sum over all the ions of terms due to the pseudopotential of each individual ion. Also, it must be symmetric in the electronic variables and linear in the number of electrons. These are nothing more than the usual conditions for any external potential acting on a system of indistinguishable particles. We state them explicitly here in order to make clear that the nonlocality of the pseudopotential in the coordinate representation of electrons does not invalidate them. Thus, the nonlocal part of the Hamiltonian must have the form

$$H_{\rm nonlocal}=\sum_{\mathbf{R}}\sum_{s,i} H^{s,i}_{\mathbf{R}}\ , \tag{37}$$

where $\mathbf{R}$ varies over the sites of the ions, s varies over the electron spin, and $i=1,N$ varies over the electrons of spin s. $H^{s,i}_{\mathbf{R}}$ is the nonlocal pseudopotential due to the ion at $\mathbf{R}$ acting on the (s,i) electron coordinates. The single-particle operator $H^{s,i}_{\mathbf{R}}$ is the translation by $\mathbf{R}$ of the nonlo-

cal pseudopotential $H^{s,i}$ of the ion situated at the origin; i.e.,

$$H^{s,i}_{\mathbf{R}} = \mathcal{T}_{\mathbf{R}}^{-1} H^{s,i} \mathcal{T}_{\mathbf{R}} , \tag{38}$$

where $\mathcal{T}_{\mathbf{R}}$ is the translation operator (acting on *all* the electronic variables) corresponding to the translation $\mathbf{R}$.

Since the total crystal nonlocal potential is a sum over the potentials of the ions, for notational simplicity we will concentrate on evaluating the energy due to a single potential centered at the origin. The sum over the crystal can then be easily done using Eq. (38) to evaluate the other terms in the nonlocal energy. The potential at the origin has the form[10]

$$H^{s,i} = \sum_l \int_0^\infty dr\, V_l(r) P^{s,i}_{l,r} . \tag{39}$$

Here $P^{s,i}_{l,r}$ is the angular momentum l projection operator acting at a distance r from the origin on the (s,i) electron variable; it is defined in coordinate representation by

$$P^{s,i}_{l,r}:\ \Psi(\mathbf{r}_1^\uparrow, \ldots, \mathbf{r}_i^s, \ldots, \mathbf{r}_N^\downarrow) \mapsto \delta(r_i^s - r) \sum_{m=-l}^{l} Y_{lm}(\Omega_{r_i^s}) \int_{r'=r} d\Omega_{\mathbf{r}'}\, Y^*_{lm}(\Omega_{\mathbf{r}'}) \Psi(\mathbf{r}_1^\uparrow, \ldots, \mathbf{r}_i^s = \mathbf{r}', \ldots, \mathbf{r}_N^\downarrow) , \tag{40}$$

where the Y_{lm} are the spherical harmonics, $\Omega_{\mathbf{r}}$ is the angular part of the spherical coordinates of $\mathbf{r}$, and $\delta(x)$ is the Dirac delta function. [The action of $H^{s,i}$ can be understood as follows: fix at particular values all the electron variables in the argument of the many-body wave function except the (s,i) variable and consider the resulting function $f(\mathbf{r}_i^s)$; the action of $H^{s,i}$ on f is precisely the same as the action of the usual (one-body) pseudopotential on single-particle wave functions in, for example, the Kohn-Sham equations.[8] This is always the way the action of a single-particle operator is generalized from the "independent-particle" situation to the "interacting-particle" case.]

The contribution of this term in the Hamiltonian to the energy of a many-body state $|\Psi\rangle$ is given by

$$E(|\Psi\rangle) = \left\langle \Psi \left| \left[\sum_{s,i} H^{s,i} \right] \right| \Psi \right\rangle = \sum_{s,i} \langle \Psi | H^{s,i} | \Psi \rangle . \tag{41}$$

Since $|\Psi\rangle$ is fully antisymmetric in the electron variables,

$$\sum_{s,i} \langle \Psi | H^{s,i} | \Psi \rangle = 2N \langle \Psi | H^{\uparrow,1} | \Psi \rangle . \tag{42}$$

So we only need to consider one term in the sum, let us say the (s,i) term:

$$E^{s,i}(|\Psi\rangle) = \langle \Psi | H^{s,i} | \Psi \rangle = \int d\mathbf{r}_1^\uparrow \int \cdots \int d\mathbf{r}_N^\downarrow\, \Psi^* H^{s,i} \Psi = \int d\mathbf{r}_1^\uparrow \int \cdots \int d\mathbf{r}_N^\downarrow\, |\Psi|^2 \left[\frac{H^{s,i}\Psi}{\Psi} \right] . \tag{43}$$

The Monte Carlo random-walk technique with importance sampling automatically integrates all quantities with respect to the weight $|\Psi|^2$. Thus, in order to calculate the one-particle energy $E^{s,i}$, we want to perform importance sampling on the quantity

$$\frac{H^{s,i}\Psi}{\Psi} .$$

Making use of Eqs. (39) and (40), we can see that the value of this function at any point $(\mathbf{r}_1^\uparrow, \ldots, \mathbf{r}_i^s, \ldots, \mathbf{r}_N^\downarrow)$ in configuration space is given by

$$\frac{\sum_l V_l(r_i^s) \sum_{m=-l}^{l} Y_{lm}(\Omega_{\mathbf{r}_i^s}) \int_{r'=r_i^s} d\Omega_{\mathbf{r}'}\, Y^*_{lm}(\Omega_{\mathbf{r}'}) \Psi(\mathbf{r}_1^\uparrow, \ldots, \mathbf{r}_i^s = \mathbf{r}', \ldots, \mathbf{r}_N^\downarrow)}{\Psi(\mathbf{r}_1^\uparrow, \ldots, \mathbf{r}_i^s, \ldots, \mathbf{r}_N^\downarrow)} . \tag{44}$$

We can simplify this expression a bit by recalling that $Y_{lm}(0,0) = 0$ for $m \neq 0$. Choosing the z axis along $\mathbf{r}_i^s$ then gets rid of the sums over m and we have the contributions from the different angular-momentum potentials $V_l(r)$ for $l = 0, 1, 2, \ldots$, as

$$E_l^{s,i}(\mathbf{r}_i^s = \mathbf{r}) = V_l(r) Y_{l0}(0,0) \int_{r'=r} Y^*_{l0}(\Omega_{\mathbf{r}'}) \frac{\Psi(\mathbf{r}_1^\uparrow, \ldots, \mathbf{r}_i^s = \mathbf{r}', \ldots, \mathbf{r}_N^\downarrow)}{\Psi(\mathbf{r}_1^\uparrow, \ldots, \mathbf{r}_i^s = \mathbf{r}, \ldots, \mathbf{r}_N^\downarrow)} d\Omega_{\mathbf{r}'} , \tag{45}$$

where $\Omega_{\mathbf{r}'}$ is the angular part of the spherical coordinates of the vector $\mathbf{r}'$ when $\mathbf{r}$ points along the z axis.

In the general case where the atom is not at the origin but at a position $\mathbf{R}^{\text{atom}}$, the nonlocal energy due to the atom consists of contributions from its different angular-momentum potentials $V_l^{\text{atom}}(r)$ for $l = 0, 1, 2, \ldots$:

$$E_l^{\text{atom},s,i}(\mathbf{r}_i^s = \mathbf{r}) = V_l^{\text{atom}}(\bar{r}) Y_{l0}(0,0) \int_{|\mathbf{r}' - \mathbf{R}^{\text{atom}}| = \bar{r}} Y^*_{l0}(\Omega_{\mathbf{r}'}) \frac{\Psi(\mathbf{r}_1^\uparrow, \ldots, \mathbf{r}_i^s = \mathbf{r}', \ldots, \mathbf{r}_N^\downarrow)}{\Psi(\mathbf{r}_1^\uparrow, \ldots, \mathbf{r}_i^s = \mathbf{r}, \ldots, \mathbf{r}_N^\downarrow)} d\Omega_{\mathbf{r}'} , \tag{46}$$

where $\tilde{r}=|\mathbf{r}-\mathbf{R}^{\text{atom}}|$ and $\Omega_{\mathbf{r}'}$ is the angular part of the spherical coordinates of the vector $\mathbf{r}'-\mathbf{R}^{\text{atom}}$ when $\mathbf{r}-\mathbf{R}^{\text{atom}}$ points along the z axis.

In principle, the expression for the energy due to one atom in Eq. (46) should be summed over *all* the atoms in the crystal to give the total nonlocal energy for electron (s,i) from Eq. (37). However, the nonlocal potentials are very short ranged ($\simeq 2$ atomic units) (Ref. 11) and so we need only sum Eq. (46) over one or two neighboring atoms in most cases.

It is immediately clear that the integral in Eq. (46) cannot be evaluated analytically and must be performed numerically. One approach would be to use a fixed grid of values for $\Omega_{\mathbf{r}'}$ and use a summation over values of the many-body wave function at those points to estimate the integral. However, this method is clearly subject to systematic bias which may converge very slowly with respect to the grid size. A more satisfactory approach in the present context is to evaluate the integral in a statistical fashion; i.e., we choose values for $\Omega_{\mathbf{r}'}$ at random according to an appropriate probability distribution and use the summation over the values of the many-body wave function at those points (with appropriate weighting factors) to obtain a statistically unbiased estimator of the integral.

The variance of such an estimator can be greatly reduced by a judicious choice of sampling scheme. We expect the many-body wave function (as a function of $\mathbf{r}'$, keeping the other electrons fixed) to have predominantly the angular-momentum character of the single-particle wave functions in the Slater determinant; viz., in most cases of interest, largely s, p, or d character. The variance of the estimator of the integral in Eq. (46) will thus be greatly reduced if the estimator is exact (i.e., has zero variance) for functions of pure s, p, or d character. Any fluctuations in the estimate of the integral will then come only from higher angular-momentum components in the many-body wave function. In Appendix C, we show how such sampling schemes can be developed to give exact evaluation of the s and p pseudopotentials for all s, p, and d wave functions.

Since the variational Monte Carlo method is intrinsically statistical in nature [even if the nonlocal integral in Eq. (46) were evaluated exactly for all functions] there is no point in evaluating Eq. (46) exactly if in doing so we expend a very large amount of computing time. In fact (see Appendix D), the optimal balance between spending time evaluating the nonlocal energy and spending time doing other computational work is reached when the ratio of time spent evaluating the nonlocal energy to time spent on other work equals the ratio of the variance of the estimator of Eq. (46) to the variance of the exact single-particle energy along the random walk.

C. The kinetic energy

Since the random-walk samples points in configuration with the probability distribution $|\Psi|^2$, the quantity we want to sample in evaluating the kinetic energy is

$$-\frac{\hbar^2}{2m}\frac{\Psi^*\nabla_i^2\Psi}{\Psi^*\Psi}=-\frac{\hbar^2}{2m}\frac{\nabla_i^2\Psi}{\Psi}\ . \tag{47}$$

To perform this evaluation we follow essentially the same procedure as in Ref. 2. Define

$$T_i\equiv-\frac{1}{2}\frac{\hbar^2}{2m}\nabla_i^2\ln\Psi\ , \tag{48}$$

and

$$\mathbf{F}_i\equiv\left[\frac{\hbar^2}{2m}\right]^{1/2}\nabla_i\ln\Psi\ . \tag{49}$$

Then it is easily shown that

$$-\frac{\hbar^2}{2m}\frac{\nabla_i^2\Psi}{\Psi}=2T_i-F_i^2\ . \tag{50}$$

From Green's theorem, it is easy to show that

$$\langle T\rangle=\langle F^2\rangle=\langle\text{kinetic energy}\rangle\ . \tag{51}$$

These relations are particularly important because they hold for *all* wave functions when sampled properly. They do *not* hold for each point along the walk and are satisfied only when the walk proceeds for a long enough time and with the correct probability distribution, viz., $|\Psi|^2$. When working with the complicated numerical wave functions of real systems they are the only exact analytic check on the internal consistency of the method. However, following Ref. 2, we do not use these relations in the evaluation of the kinetic energy itself. Rather, we explicitly evaluate the kinetic energy from Eq. (50) because the variance of this quantity is much smaller than variance of F^2 or T.

To evaluate T_i and F_i^2 we need to consider the specific form of the many-body wave function,

$$\Psi=\Psi_J d\ ,$$

where Ψ_J is the Jastrow factor and d is the Slater determinant,

$$d=d_{\text{old}}q=d_{\text{old}}\sum_{j=1}^{N}\tilde{D}^{s}_{ji,\text{old}}\phi_j(\mathbf{r}_i^s)\ , \tag{52}$$

where d_{old} is the Slater determinant for the previous positions of the electrons (*not* the trial positions, where the kinetic energy is to be evaluated). Note that neither d_{old} nor $\underline{\tilde{D}}^{s}_{\text{old}}$ depend on $\mathbf{r}_i$.

Then

$$\nabla_i\ln\Psi=\nabla_i\ln\Psi_J+\nabla_i\ln d=\nabla_i\ln\Psi_J+\frac{1}{d}\nabla_i d=\nabla\chi(\mathbf{r}_i^s)-\sum_{(s',j)\neq(s,i)}\nabla_i u(r_{ij})+\frac{1}{q}\sum_{j=1}^{N}\tilde{D}^{s}_{ji,\text{old}}\nabla_i\phi_j(\mathbf{r}_i^s)\ , \tag{53}$$

and

$$\nabla_i^2 \ln\Psi = \nabla_i^2 \ln\Psi_J + \nabla_i^2 \ln d = \nabla_i^2 \ln\Psi_J - \left[\frac{1}{d}\nabla_i d\right]^2 + \frac{1}{d}\nabla_i^2 d$$

$$= \nabla^2\chi(\mathbf{r}_i^s) - \sum_{(s',j)\neq(s,i)} \nabla_i^2 u(r_{ij}) - \left[\frac{1}{q}\sum_{j=1}^{N} \tilde{D}^{s}_{ji,\text{old}} \nabla_i \phi_j(\mathbf{r}_i^s)\right]^2 + \frac{1}{q}\sum_{j=1}^{N} \tilde{D}^{s}_{ji,\text{old}} \nabla_i^2 \phi_j(\mathbf{r}_i^s) \ . \quad (54)$$

Since we have analytic expressions for χ [in terms of its Fourier components, as in Eq. (21)], u [from Eqs. (15) or (17)], and for the ϕ_j [in terms of their Gaussian and/or plane-wave expansion, as in Eqs. (27) and (28)], ∇ and ∇^2 of these quantities have corresponding analytic expressions which are used to calculate them in Eqs. (53) and (54). The two-body term $u(r_{ij})$ is summed over the infinite array of images of j for crystalline calculations, and so its evaluation involves an Ewald sum for the $1/r$ part, as discussed in Sec. IV D below for the electron-electron interaction. In calculating ∇u and $\nabla^2 u$, the analytic expressions for the derivatives of the Ewald sums are used.

D. The electron-electron interaction

In keeping with the periodic boundary conditions imposed on the wave function in Sec. III, we would like to have an electron-electron interaction which also has periodic behavior when the simulation region is periodically extended to all space.[39] We imagine that each electron (and each ion) in the simulation region has an infinite array of images in space. The simulation region is then a super cell for each of these arrays. The interaction of particle i with particle j is then defined to be the electrostatic interaction of the electronic charge at position i in the simulation region with electronic charges at the infinite array of image positions of particle j (including the one in the simulation region itself):

$$V(i,j) = \sum_{\mathbf{S}} \frac{e^2}{|(\mathbf{S}+\mathbf{r}_j)-\mathbf{r}_i|} \quad \text{for } i\neq j \ , \quad (55)$$

where $\mathbf{S}$ varies over the superlattice for repetition of the simulation region. As it stands, this sum does not converge for the infinite lattice. However, we handle such lattice sums in the same way as in evaluating the local potential in Sec. IV A; i.e., we add a neutralizing positive background to the sum over images of j to get an Ewald sum for the interaction potential.

Upon Fourier transform, the potential in Eq. (55) gives the usual expression for the exchange energy[49] in a box with periodic boundary conditions,

$$E_x = \frac{1}{2}\frac{1}{N}\sum_{\mathbf{k}} n_{\mathbf{k}} \left[-\frac{1}{V}\sum_{\mathbf{k}'} \frac{4\pi e^2}{|\mathbf{k}-\mathbf{k}'|^2} n_{\mathbf{k}'}\right] , \quad (56)$$

where $n_{\mathbf{k}}$ is the number operator for a plane-wave state $\mathbf{k}$ which is compatible with the periodic boundary conditions on the simulation region, and V is the volume of the region.

We must add another term to the electron-electron energy which corresponds to an interaction of particle i with its own images:

$$V(i,i) = \sum_{\mathbf{S}\,(\neq 0)} \frac{e^2}{|\mathbf{S}|} \ . \quad (57)$$

This term goes to zero in the limit of an infinite simulation region. We introduce it in our Hamiltonian because when the simulation region is finite, it gives a better approximation to the properties of the infinite system.

To see this, we note that if we use an electron-electron interaction given by Eq. (55) alone [without the "self-image" term of Eq. (57)] the depletion of the charge density near the electron i due to exchange and correlation in the many-body wave function is periodically repeated on the lattice of the simulation region. Thus we get, not only the electrostatic interaction of the electron with its own "exchange-correlation hole," but with an infinite array of images of this hole. Recall that, in the uniform electron gas, the electron-electron energy is the electrostatic interaction energy of an electron with this charge depletion:[50]

$$E_{\text{el-el}} = \int \frac{e^2}{2r}[1-g(\mathbf{r})]\, n(\mathbf{r})\, d\mathbf{r} \ , \quad (58)$$

where $g(\mathbf{r})$ is the pair-correlation function and $n(\mathbf{r})$ is the density. If the exchange-correlation hole is spherical and completely contained within one simulation region, the "self-image" term given by Eq. (57) exactly cancels the electron interaction with all the image holes outside the simulation region. In general the exchange-correlation hole will not be spherical or may not be entirely contained within one simulation region and, even with the introduction of the self-image term, there will be dipole, quadrupole, and higher multipole electrostatic interactions with the image holes. However, even in these cases, the energy per particle of the finite system with the self-image correction is much closer to that for the infinite system than it is without the self-image term.

In practice, the electron-electron energy is evaluated by the Ewald summation technique:[48]

$$E_{\text{el-el}}(\mathbf{r}_i^s) = \tfrac{1}{2}\sum_{(s',j)} V(\mathbf{r}_i^s, \mathbf{r}_j^{s'}) = \tfrac{1}{2}\Sigma_{\text{Ewald}} \ , \quad (59)$$

where the Ewald sum Σ_{Ewald} is given by

$$\sum_{\substack{\mathbf{S},s',l \\ (s',l)\neq(s,i)}} V^R[|(\mathbf{S}+\mathbf{r}_l^{s'})-\mathbf{r}_i^s|] + \sum_{\mathbf{k}} V^F(\mathbf{k})[\rho(\mathbf{k})\exp(i\mathbf{k}\cdot\mathbf{r}_i^s)-1]+C_0 \ . \quad (60)$$

The sum on $\mathbf{k}$ is over the reciprocal lattice corresponding to the simulation superlattice. The Fourier transform of the charge of the electrons is

$$\rho(\mathbf{k}) = \sum_{(s,j)=(\uparrow,1)}^{(\downarrow,N)} \exp(-i\mathbf{k}\cdot\mathbf{r}_j^s) \ . \quad (61)$$

As in Sec. IV A, the "real-space" potential V^R is the usual $1/r$ potential multiplied by an erfc function:

$$V^R(r)=\frac{e^2\mathrm{erfc}(\sqrt{\alpha}r)}{r} . \tag{62}$$

The "Fourier-space" terms are given by

$$V^F(\mathbf{k})=\begin{cases}\dfrac{4\pi e^2\exp(-k^2/4\alpha)}{k^2V} & \text{for } \mathbf{k}\neq 0\\ -\dfrac{\pi e^2}{V\alpha} & \text{for } \mathbf{k}=0 .\end{cases} \tag{63}$$

The "self-image" term is given by

$$C_0=\sum_{\mathbf{S}\,(\neq 0)} V^R(|\mathbf{S}|)+\sum_{\mathbf{k}} V^F(\mathbf{k})-2\sqrt{(\alpha/\pi)} . \tag{64}$$

The converged value of the Ewald sum is independent of α. The value of α is chosen to give equivalent convergence in real and Fourier space, as in Sec. IV A.

V. RESULTS AND COMPARISON TO EXPERIMENT

A. Atoms

We have applied the method described above to determine the ionization energy and electron affinity of atomic carbon and silicon. Calculations were carried out for the total energy of the neutral, positively, and negatively charged atoms. In each case, we fixed the parameter a in the two-body term $u(r_{ij})$ in the Jastrow factor using the cusp condition and searched the b,α parameter space to determine the optimal u and χ functions to minimize the total energy. Since the atoms are spin polarized, we have different χ functions for different spin types.

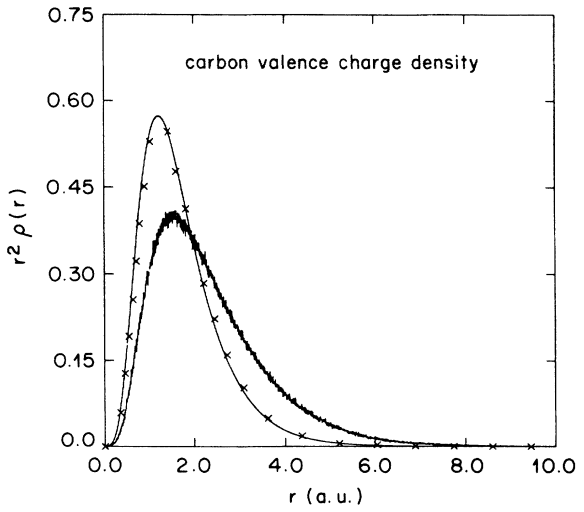

FIG. 1. Calculated valence electron charge density of the carbon atom. The solid line is the LDA calculated result; the jagged curve is the QMC result with the two-body term $u(r_{ij})$ only in the Jastrow factor; the crosses are the QMC results calculated with both the one- and two-body terms [$\chi(\mathbf{r}_i)$ and $u(r_{ij})$] included in the Jastrow factor (see text).

For the atoms considered, we find that both the one-body and two-body terms are equally important in lowering the energy of the system when compared to that of the single Slater determinant wave function. Without the one-body term $\chi(\mathbf{r})$ in the Jastrow factor, the presence of a nonzero $u(r_{ij})$ significantly alters the charge density from that of the Slater determinant alone. This is illustrated in Fig. 1 for carbon. Since the correlation term $u(r_{ij})$ reduces the probability of two electrons getting close to each other, its effect is to reduce the charge density in the high-density regions and increase it in the low-density regions. The resulting charge density is then too diffuse as compared to experiment. As seen in Fig. 1, the optimal one-body term $\chi(\mathbf{r})$ brings the charge density back to a distribution which is very close to the LDA result. For neutral carbon, the one-body term lowers the energy of the atom by 1.8 eV, compared to the optimized energy for a Jastrow factor with the two-body term only. The optimal values of the parameters in the two-body term of the Jastrow factor are substantially different with and without the one-body term since different two-body terms affect the charge density differently. The lowering of energy due to the one-body term keeping the two-body term constant at the final optimal parameters (i.e., the lowering in energy due to the change of the charge density shown in Fig. 1) is 4.5 eV in the neutral carbon atom.

We present in Table I the calculated ionization energies and electron affinities together with experimental results. Both C^- and Si^- are unbounded in the LDA. This has forced us to take a somewhat different approach to the generation of the single-particle orbitals; since we cannot generate LDA wave functions for the negative ion, instead we have used single-particle wave functions generated from a Hartree-Fock calculation for the valence electrons only, with the same (LDA generated) atomic pseudopotentials as for all the other calculations. These single-particle wave functions are then used in the Monte Carlo calculation for the negative ion. In all the LDA calculations a spherically symmetrized potential is used to solve for the single-particle states. The present approach gives values in good agreement with experiment to within ± 0.15 eV. The calculated second and third ionization potentials differ more from experiment, but one does not expect transferability of the pseudopotential over so large an energy range.

We also tried a scheme for generating single-particle wave functions for the negative ion where we fractionally

TABLE I. Ionization energy and electron affinity of atomic carbon and silicon (in eV). The expected statistical error in the last digits is in parentheses.

	Variational QMC	Experiment[a]
Carbon ionization energy	11.43(5)	11.26
Electron affinity	1.20(10)	1.27
Silicon ionization energy	8.20(5)	8.15
Electron affinity	1.40(10)	1.39

[a]Reference 15.

TABLE II. Terms in the total energy of the solid (64-electron simulation at a lattice constant $a = 3.63$ Å) for a single Slater determinant of LDA wave functions and for a Jastrow-Slater function with a two-body term *only* in the Jastrow factor, as discussed in the text, and with LDA wave functions in the determinant. Energies in eV/atom.

	Slater determinant	Jastrow-Slater (u only)
Local potential	−87.1	−73.6
Electron-electron	−29.2	−39.0
Kinetic	121.3	116.8
Nonlocal potential	15.8	12.8
Ewald sum	−171.0	−171.0
Total	−150.2	−154.0

occupied the states in the LDA calculation so that the total ionic charge is −0.5, this being the largest negative charge for which the LDA produces bound wave functions. However, this scheme yielded less satisfactory wave functions, giving electron affinities for C and Si of 1.05±0.10 eV and 1.2±0.1 eV, respectively. This sensitivity of the electron affinity results to the single-particle wave functions clearly reflects the need for appropriate and accurate single-particle wave functions in the Slater determinant.

We note that since the number of three-body interactions is very different for these atoms in the three different charge states shown, our results show that three-body terms in the Jastrow factor appear to be not significant at the level of accuracy of the pseudopotential approximation itself, and can lower the energy by no more than approximately 0.2 eV/atom. A similar conclusion is suggested by comparison of our results for the Si atom with those from the Green's-function Monte Carlo pseudo-Hamiltonian calculation of Bachelet, Ceperley, and Chiocchetti.[14] The absolute energy of our LDA calculation is lower by 0.04 eV than their pseudo-Hamiltonian LDA result for the silicon atom[51] (the two pseudopotentials are not identical). Our variational Monte Carlo calculation with the pseudopotential is only 0.15 eV higher in energy for the atom than the Green's-function Monte Carlo calculation with the pseudo-Hamiltonian. Allowing for the fact that the two many-body Hamiltonians are not identical, nevertheless, it is reasonable to conclude that the amount of correlation energy absent in the variational wave function of the form we have used is no more than 0.1–0.2 eV/atom.

B. Graphite and diamond

The method has been applied to study the binding energy and structural properties of diamond and graphite using simulation cells with periodic boundary conditions, as described above. Cell sizes containing up to 216 electrons (or 54 carbon atoms) were used. It is found that the size dependence for larger simulations is mainly determined by the convergence of the single-particle terms in the total energy, as given in LDA band theory by the **k**-point sampling of the Brillouin zone.

Table II presents the results for a specific simulation showing the various contributions to the total energy of diamond. As seen from the table, inclusion of a Jastrow factor with only the two-body term $u(r_{ij})$ lowers the total energy of the solid by 3.8 eV/atom. With the introduction of the Jastrow factor, the electron-electron energy is substantially reduced as expected because of the added correlation among the electrons. However, contrary to findings in uniform systems, the kinetic energy is also decreased. It is the electron-ion interaction energy which is greatly increased. The general trends in the atoms, graphite and silicon are similar. This difference in behavior in the kinetic energy may be understood in terms of the effect of $u(r_{ij})$ on the wave function in the bonding region where the charge density is high. Distributing the charge density away from these regions leads to both a decrease in the kinetic energy and an increase in the electron-ion energy. The introduction of the one-body term into the Jastrow factor further lowers the energy of diamond, but only by 0.3 eV/atom, compared to 4.5 in the carbon atom (as discussed above). In diamond, the optimum parameters in the two-body term do not depend significantly on the presence or absence of the one-body term. In graphite, where the charge density is substantially more susceptible to change by the two-body term in the Jastrow factor (due to the presence of large, very low density regions in the interlayer region) the lowering of the energy by the one-body term χ is 4.2 eV/atom, much larger than in diamond. Thus we see that the influence of

TABLE III. Total energies (in eV/atom) of the carbon pseudoatom and of diamond (with finite-size correction) for (a) the LDA calculation, and for Monte Carlo calculations with (b) a single Slater determinant of LDA wave functions, and (c) the Jastrow-Slater function with one- and two-body terms in the Jastrow factor. The experimental cohesive energy results (d) are adjusted to allow for the zero-point phonon energy (0.18 eV/atom) of the solid. The expected statistical error in the last digits is in parentheses.

	Carbon atom	Diamond	Cohesive energy
(a) LDA	−146.79	−155.42	8.63
(b) Slater determinant	−145.55(7)	−151.3(2)	5.85(25)
(c) Jastrow-Slater	−147.93(3)	−155.38(6)	7.45(7)
(d) Experiment[a]			7.37

[a]See Ref. 19.

the one-body term on the energy varies greatly from system to system.

The total energies calculated with and without the full Jastrow factor (i.e., both the u and χ terms are included) in the wave function are presented in Table III for diamond at the minimum-energy lattice constant together with the atomic results. The QMC results for the solid include a finite-size correction beyond the 216-electron simulation obtained from the difference between the LDA energy calculated using **k** points compatible with periodic boundary conditions on this simulation region and that calculated with a fully converged **k**-point set. This energy difference is 0.2 eV/atom. We have found that the finite-size correction to the QMC energy calculations for regions containing between 64 and 216 electrons follows within 20% that of the corresponding LDA calculation. This fact merely demonstrates the relatively localized nature of the exchange-correlation hole in this system. We also include the phonon zero-point energy of 0.18 eV/atom in the energy of the diamond crystal. Using the Slater-determinant-only results as Hartree-Fock energies, we obtain for the correlation energies of the valence electrons in the atom and the solid the values of 2.4 ± 0.1 eV and 4.1 ± 0.2 eV/atom, respectively. This is in agreement with calculations[36] for the valence electron correlation energies in a tight-binding calculation using a similar *ansatz* for the many-body wave function, but evaluating the energy by diagrammatic techniques. Our result for the Hartree-Fock cohesive energy of 5.85 ± 0.25 eV/atom is also in agreement with the results of Ref. 36.

Also present in Table III is the cohesive energy of diamond calculated using the present approach together with the LDA value using the Ceperley-Alder form[3,52] for the exchange-correlation energy as parametrized by Perdew and Zunger and the experimental number. The quantum Monte Carlo calculation gives a cohesive energy of 7.45 ± 0.07 eV/atom, as compared to the experimental value of 7.37 eV/atom. This result is in significantly better agreement with experiment than the LDA value of 8.63 eV/atom. (Typically, LDA binding energies are too large[9] as compared to experiment by 15–20 %.) The very close agreement between the LDA and QMC total energies for diamond seems to be fortuitous, in the light of the corresponding result for silicon (see below) and should not be used to draw the conclusion that the error in the LDA binding error comes *in general* from an error in the atomic energy only.

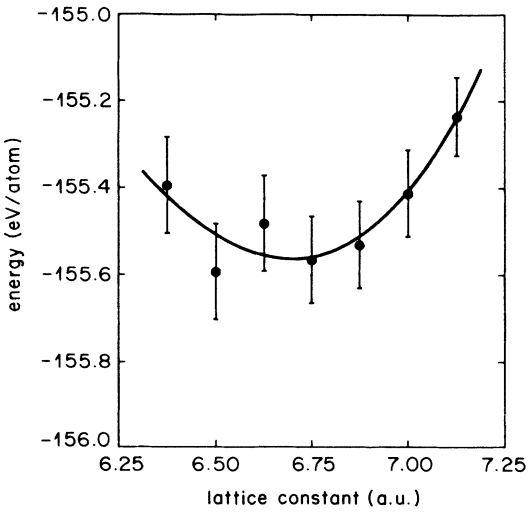

FIG. 2. Calculated total energy of diamond as a function of the lattice constant. The curve is a fit of the Murnaghan equation of state to the calculated points. The error bars indicate the standard deviation of the mean in each Monte Carlo calculation.

Figure 2 shows the calculated total energy of diamond as a function of lattice constant. The theoretical points are fitted with a Murnaghan equation of state[53] (the solid line). The resulting structural parameters are shown in Table IV, along with those of silicon. These results for the structural properties are within one standard deviation of the experimental values[54,55] and are at the same level of accuracy as the LDA, which was already very successful[56] in predicting the equation of state of diamond. The pressure derivative of the bulk modulus is not reliably estimated from the present calculation, due to statistical noise in the energies.

Since the electronic and geometric structure of graphite, which is a highly anisotropic semimetal with very large inhomogeneity of charge density, differ substantially from those of diamond, the calculation of its cohesive energy represents a significantly different challenge to the present method. In particular, one might wonder in advance whether the spherically symmetric and translationally invariant form of the two-body term of the Jastrow factor in our wave function would be an adequate approximation for graphite. As we have already mentioned, the effect of the one-body term on the total energy is an order of magnitude greater in graphite than it is in diamond. However, our result for the cohesive energy is in excellent agreement with experiment. We obtain a QMC cohesive energy for graphite that is identical to the calculated diamond cohesive energy, within the statistical noise of 0.07 eV/atom. The measured cohesive energy of graphite is found to be only 0.025 eV/atom larger than that of diamond.[19]

We have not been able to reliably estimate the correlation energy in graphite because of difficulty of obtaining a

TABLE IV. Calculated lattice constants and bulk moduli for diamond and silicon. The expected statistical errors in the last digits of the calculated numbers are in parentheses.

	a_0 (Å)	B_0 (GPa)
	Diamond	
Present calc.	3.54(3)	420(50)
Expt.	3.567[a]	443[b]
	Silicon	
Present calc.	5.40(4)	108(10)
Expt.	5.430[c]	98.8[c]

[a]Reference 54.
[b]Reference 55.
[c]Reference 58.

TABLE V. Total energies (in eV/atom) of the silicon pseudoatom and of silicon solid (with finite-size correction) for (a) the LDA calculation, and for Monte Carlo calculations with (b) a single Slater determinant of LDA wave functions and (c) the Jastrow-Slater function with one- and two-body terms in the Jastrow factor. The experimental cohesive energy results (d) are adjusted to allow for the zero-point phonon energy (0.07 eV/atom) of the solid. The expected statistical error in the last digits is in parentheses.

	Silicon atom	Solid	Cohesive energy
(a) LDA	−102.76	−108.05	5.29
(b) Slater determinant	−101.34(7)	−105.0(1)	3.66(13)
(c) Jastrow-Slater	−103.42(3)	−108.30(6)	4.88(7)
(d) Experiment			4.84(13)[a]
			4.71(03)[b]
			4.77(13)[c]
			4.62[d]
			4.76[e]
			4.97(13)[f]

[a]Reference 20.
[b]Reference 21.
[c]Reference 22.
[d]Reference 23.
[e]Reference 24.
[f]Reference 25.

converged Hartree-Fock energy within the present scheme. Although the finite-size correction of the full QMC calculation (with both Jastrow factor and Slater determinant) follows that of the LDA calculations with great accuracy, this is not true of the QMC calculation using the Slater determinant only. This is due to the singular nature of the Hartree-Fock self-energy near the Fermi level,[57] a problem which does not arise in the insulating diamond structure. As is well known,[49] the introduction of correlation removes this unphysical anomaly in the self-energy. In this sense the LDA behavior is much closer to the correlated wave function.

C. Silicon

We have calculated the cohesive energy and structural properties of silicon following the same procedure as for diamond. The results for the cohesive energy are summarized in Table V. The energy of the solid as a function of atomic volume is shown in Fig. 3 and is fitted to a Murnhaghan equation of state. The structural parameters resulting from the fit, shown in Table IV, are in excellent agreement with experiment,[58] as are the values obtained from LDA calculations.

Due to the scatter in the experimental results for the cohesive energy, silicon provides a less stringent test of the present calculation than does diamond. Thus, although the calculated number is within the range of the experimental results, we cannot say for sure if the combination of LDA pseudopotentials with variational many-body wave functions is as satisfactory in the solid for silicon as it is for carbon.

It is likely that the larger core of silicon renders the pseudopotential approximation less accurate there than in carbon, but, even within the framework of LDA calculations only, this effect is hard to estimate accurately[59] because of the various numerical approximations employed in pseudopotential and all-electron LDA calculations. Moreover, the pseudopotential may not be as transferrable between different environments in many-body calculations as it is in LDA calculations. Our "Hartree-Fock" cohesive energy (obtained from the difference between the single Slater determinant results for the atom and the crystal) is 3.66±0.12 eV/atom, in

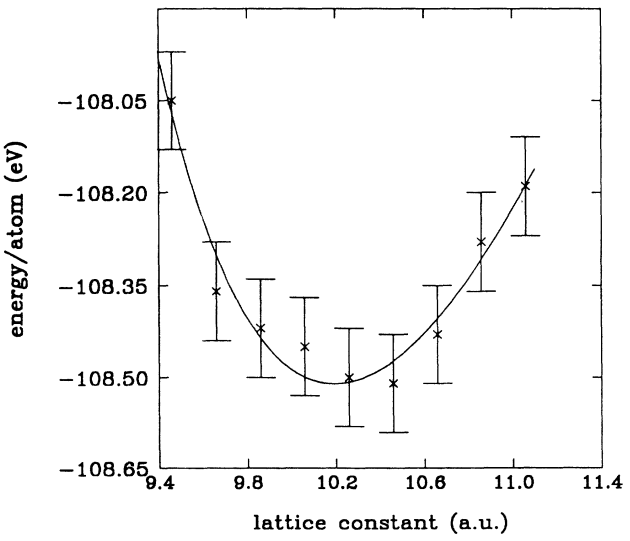

FIG. 3. Calculated total energy of silicon as a function of the lattice constant. The curve is a fit of the Murnaghan equation of state to the calculated points. The error bars indicate the standard deviation of the mean in each Monte Carlo calculation.

good agreement with other Hartree-Fock calculations for silicon,[60] but unfortunately these are also performed with a pseudopotential approximation.

The correlation energy for the silicon atom in the present calculation (obtained from the difference between the energy of the single Slater determinant wave function and that of the Jastrow-Slater wave function) is 2.1 eV/atom, compared with a value of 1.81 eV/atom from a recent calculation[60] using coupled-cluster diagrammatic techniques and a local-orbital basis. The effects of finite basis size on the calculation is estimated in Ref. 60 to be 0.6 eV/atom, giving an "infinite basis" limit of 2.41 eV/atom. The correlation energy of the silicon crystal obtained in the present calculation is 3.5 eV/atom, compared with a finite-basis result from Ref. 60 of 2.61 eV/atom. The finite basis correction for the result in Ref. 60 is estimated to be 0.98 eV/atom, giving an infinite basis limit of 3.59 eV/atom.

In the light of a review of the original experimental results (in particular, the most recent result), the "recommended value" for the cohesive energy of silicon quoted in the JANAF tables[61] seems low and its quoted uncertainty optimistically small (see the scattered data in Table V). The cohesive energy is derived from the heat of sublimation and other thermodynamic data. However, sublimation rates are affected by surface contaminants[21,24] and the partial pressure of elemental silicon is difficult to measure accurately.[22] Aside from the quoted statistical uncertainties, systematic errors are difficult to eliminate, or even to assess, in these experiments. Since the most recent measurement of the heat of sublimation was in the early 1970's, it would be interesting if developments in vacuum techniques and sample preparation since that time would now allow a more accurate determination of the cohesive energy of silicon.

VI. CONCLUSION

In conclusion, we have developed a scheme for the calculation of total energies of the valence electrons in atoms and solids using nonlocal pseudopotentials in conjunction with variational quantum Monte Carlo techniques. We find that a correlated many-body wave function of surprisingly simple form can yield 90–95 % of the correlation energy in the carbon- and silicon-based systems studied. The results give excellent agreement with experimental energy differences for carbon-based systems. The structural properties are also in good agreement with experiment. For silicon, the results are similarly in excellent agreement with experiment.

The computational effort involved in these QMC solid-state calculations is approximately 5–10 times that of the corresponding LDA calculation. (One lattice constant for diamond in Fig. 2 takes about one hour on a single-processor Cray X-MP supercomputer.) This ratio is of course strongly dependent on the size of the crystal unit cell. The LDA computation grows roughly as the cube of the cell size, while the QMC computation grows roughly linearly with cell size.

With the full many-body wave function available, it is clear that many quantities other than the energy may be calculated. In particular, quantities inaccessible in the LDA approach, such as pair-correlation functions and single-particle occupation numbers, can be readily calculated in the present method. Work is continuing with this method to extend the total-energy calculations to transition-metal systems and also to calculate pair-correlation functions, Compton profiles, and quasiparticle energies within a variational many-body approach.

ACKNOWLEDGMENTS

We wish to thank D. Ceperley for communicating some of their unpublished Green's-function Monte Carlo results for atomic silicon, and J. C. Phillips and D. R. Hamann for numerous helpful discussions. This work was supported by the National Science Foundation Grant No. DMR-83-19024 and by the Director, Office of Energy Research, U.S. Department of Energy (Materials Sciences Division of the Office of Basic Energy Sciences) under Grant No. DE-AC03-76SF00098. One of us (X. W. W.) would like to acknowledge the support of the Center for Advanced Materials and another (S.G.L.) the support of the Guggenheim Foundation (New York, NY). Cray computer time was provided by the Office of Energy Research of the U.S. Department of Energy and by the National Science Foundation at the San Diego Supercomputer Center.

APPENDIX A: CALCULATION OF THE ONE-BODY JASTROW TERM χ

The charge density ρ for any of the many-body wave functions must itself be statistically estimated and care must be taken to eliminate noise from the resulting function χ. In the atoms, the function χ is taken to be spherically symmetric (even though the atoms considered are open-shell systems), and the angle-integrated charge on each interval of a uniform radial grid of several thousand points is calculated over a random walk for each of two many-body wave functions (e.g., with and without the factor χ). The ratio of the charges on the intervals for the two different many-body wave functions is then calculated. The logarithm of this ratio is smoothed by a seventh-order polynomial fit through the points giving the final χ which is scaled then by the variational parameter α. For the iterated χ, it is the final sum over χ_i, rather than the individual χ_i, which is smoothed. This gives better numerical stability of the final result.

In the solid, the smoothing is done in Fourier space. The Fourier components of the charge density for vectors in Fourier space on the reciprocal lattice of the crystal up to a cutoff length are accumulated over a random walk for each many-body wave function. For each point on the walk and each reciprocal-lattice vector $\mathbf{G}$, the Fourier transform $\exp(-i\mathbf{G}\cdot\mathbf{r}_i)$ of the position $\mathbf{r}_i$ of the particle being moved is accumulated. The resulting charge is then symmetrized according to the known symmetry point group of the crystal by averaging the values obtained for symmetry-related Fourier components in the walk average. (Note that although the true charge density of the many-body ground-state wave function has the

full crystal symmetry, the estimate of this quantity obtained over any *particular* random walk will not.) Finally, the symmetrized charge is smoothed by multiplying the resulting Fourier components for vectors of length g by a Gaussian decay factor, $\exp(-\gamma g^2)$. This smoothing is equivalent to replacing the δ-function of charge density $\rho(\mathbf{r})=\delta(\mathbf{r}-\mathbf{r}_i)$ in real space which comes from each particle along the random walk by a normalized Gaussian $\rho(\mathbf{r})=(4\pi^2\gamma)^{-3/2}\exp(-|\mathbf{r}-\mathbf{r}_i|^2/4\pi\gamma)$. The logarithm of the ratio of the two smoothed charge densities is calculated by fast-Fourier transform of the densities to real space, where the ratio and logarithm is calculated at each point on the transform grid. The resulting function is transformed back to Fourier space again so that χ which is finally used in the many-body wave functions is represented in Fourier space:

$$\chi(\mathbf{r})=\sum_{\mathbf{G}}\chi(\mathbf{G})\exp(i\mathbf{G}\cdot\mathbf{r}) . \tag{A1}$$

The value of γ is determined variationally to minimize the total energy of the solid. In the case of diamond and graphite, γ has an optimal value of 0.1 in atomic units; in silicon its optimal value is 0.18 a.u. The total energy varies by no more than 0.1 eV with variations of γ up to 50% from these values.

APPENDIX B: UNBIASED SAMPLING OF THE ENERGY PER PARTICLE

Although this seems like a very straightforward process, subtle errors can arise if we are not careful about the *precise* way in which we sample the energy. Sometimes, a sampling algorithm which seems intuitively correct will give biased answers.

Consider the following algorithm.

Each particle is updated in turn (particle 1 first, particle 2 second, etc., and when we update the last particle, we go through the list again). If the move is accepted, we evaluate the energy of the particle being moved, say the ith particle of spin s, and add it to the average; if the move is rejected, we keep the *last calculated* single-particle energy [which, in general, is not the energy of the (s,i) particle in the old configuration], and add *it* to the average. Thus, we have an *old* energy and a *new* energy. The new energy is the energy of the particle being moved at its new (trial) position. If the move is accepted the "old" energy is set equal to the new energy, otherwise it is unchanged. The average is always updated with the "old" energy, after the move has been accepted or not accepted.

What is wrong with this algorithm?

The problem here is that the energy of particle i at position $\mathbf{r}_i^s$ only enters the list for the average if the configuration $\{\mathbf{r}_j^{s'}\}_{(s',j)=(\uparrow,1)}^{(\downarrow,N)}$ has been reached by a process where particle (s,i) is the *last* to be moved. The energy of a particle at $\mathbf{r}_i^s$ is never included when we end up at configuration $\{\mathbf{r}_j^{s'}\}_{(s',j)=(\uparrow,1)}^{(\downarrow,N)}$ by rejecting a change in the position of $\mathbf{r}_i$.

Let us calculate the probability density of getting a configuration $R\equiv\{\mathbf{r}_j^{s'}\}_{(s',j)=(\uparrow,1)}^{(\downarrow,N)}$ *and* using particle (s,i) as the particle whose energy is evaluated, according to the given algorithm. For unbiased sampling, this probability density should be $|\Psi(R)|^2/2N$. [This result arises from the assumptions that the walk is at equilibrium and that the configuration probability density is correct, i.e., $=|\Psi(R)|^2$. Since we move each particle in turn, the probability that we are moving particle (s,i) at any given (randomly selected) point in the walk is $1/2N$.] Let V be the volume around $\mathbf{r}_i^s$ from which it is possible to move in a single step to $\mathbf{r}_i^s$. (This is a cube of side twice the maximum step length.) The probability density of choosing a trial position in a volume V around the old position $\mathbf{r}'$ is uniform, and so the probability density of choosing position $\mathbf{r}_i^s$ as a trial position is $1/V$ when $\mathbf{r}'$ lies in the volume V around $\mathbf{r}_i^s$. Once $\mathbf{r}_i^s$ is chosen as a trial position, we decide whether to accept it or not according to the usual rule. If we accept it, we add the energy at $\mathbf{r}_i^s$ in the configuration R to the energy average. Thus, the probability density of evaluating the energy at $\mathbf{r}_i^s$ in the configuration R by a final move of particle (s,i) is equal to

$$\begin{aligned}\int d\mathbf{r}'\,|\Psi(\mathbf{r}_1^{\uparrow},\ldots,\mathbf{r}_i^s=\mathbf{r}',\ldots,\mathbf{r}_N^{\downarrow})|^2P(\mathbf{r}'\to\mathbf{r}_i^s)&=\int_V d\mathbf{r}'|\Psi(\ldots,\mathbf{r}',\ldots)|^2\min\left\{1,\left|\frac{\Psi(\ldots,\mathbf{r}_i^s,\ldots)}{\Psi(\ldots,\mathbf{r}',\ldots)}\right|^2\right\}\frac{1}{V}\frac{1}{2N}\\&=\frac{1}{2NV}\int_V d\mathbf{r}'\min\{|\Psi(\ldots,\mathbf{r}_i^s,\ldots)|^2,|\Psi(\ldots,\mathbf{r}',\ldots)|^2\}\\&\le\frac{1}{2N}|\Psi(\ldots,\mathbf{r}_i^s,\ldots)|^2 .\end{aligned} \tag{B1}$$

Equality occurs in the last part of Eq. (B1) only if the probability density at R is less than that at all configurations which can be reached from R by one step. We will continue to include the energy of particle (s,i) into the energy averages in subsequent moves of the walk if we *reject* the trial positions of particle $(s,i+1)$, $(s,i+2)$, etc. This will enhance the probability density of evaluating the energy at $\mathbf{r}_i^s$ in configuration R, clearly giving too large a value when equality occurs in the last part of Eq. (B1). In general, the probability given in Eq. (B1), enhanced by the rejection of subsequent moves, will not equal $|\Psi(R)|^2/2N$. Roughly speaking, the sampling process biases against a point $\mathbf{r}_i^s$ which has points of lower probability density nearby.

The correct algorithm is to set the "old" energy equal to the energy of the (s,i) particle in its old position if the move is rejected, and equal to its energy in its new position if the move is accepted. The probability density of being at configuration R and *rejecting* a move of particle (s,i) equals

$$|\Psi(R)|^2\frac{1}{2N}\left[1-\int_V P(\mathbf{r}_i^s\rightarrow\mathbf{r}')d\mathbf{r}'\right]=\frac{1}{2N}|\Psi(\ldots,\mathbf{r}_i^s,\ldots)|^2-\frac{1}{2NV}\int_V d\mathbf{r}'\min\{|\Psi(\ldots,\mathbf{r}_i^s,\ldots)|^2,|\Psi(\ldots,\mathbf{r}',\ldots)|^2\}\ . \tag{B2}$$

The sum of the probability densities on the right-hand side of Eqs. (B1) and (B2) always equals $|\Psi(R)|^2/2N$, and so the "correct" algorithm does indeed sample the energy correctly.

APPENDIX C: STATISTICAL INTEGRATION OF THE NONLOCAL PSEUDOPOTENTIAL

We will develop in this appendix a scheme for randomly selecting a grid of n points, $\{\Omega_i\}_{i=1}^n$, on the unit sphere and associated weights, $\{W_i\}_{i=1}^n$, for use in the projection of the lth angular-momentum component of an arbitrary function. The grid is to have the following properties:

1. The sum over the grid points of any function defined on the unit sphere will give an *unbiased estimator* of the integral of the function over the sphere; i.e.,

$$\left\langle\sum_{i=1}^n W_i f(\Omega_i)\right\rangle=\int f(\Omega)\,d\Omega\ , \tag{C1}$$

where the notation $\langle\ \rangle$ denotes the average value taken over grids chosen at random according to the selection scheme.

2. The grid scheme for integration of the l angular-momentum potential is to be *exact* for projection of functions of angular momentum up to $l_{\max}$ in the following sense: the relation

$$\sum_{i=1}^n W_i Y_{l0}^*(\Omega_i)Y_{l'm}(\Omega_i)=\delta_{ll'}\delta_{0m} \tag{C2}$$

is to be satisfied exactly for *any* particular grid chosen, for values of l' up to $l_{\max}$ and m between $-l'$ and l'.

The first condition tells us that the average of the estimator is correct for *all* functions and the second condition that the variance of the estimator is zero for functions of angular momentum less than or equal to $l_{\max}$.

We can achieve the first objective by taking *any* fixed grid of points on the sphere with fixed weights summing to unity and rotating the coordinate axes in which the set is fixed so that the rotated z axis has a uniform solid angle distribution and the final x and y axes are rotated with a uniform planar angle about the final z axis. The grid in this rotated set of axes is used to evaluate the average in Eq. (C1). It is easy to show that each point of the original grid covers the entire sphere with a uniform solid angle distribution by this rotation scheme. Thus the integration scheme samples all functions without bias.

In order to achieve exact angular momentum l of all functions up to angular momentum l', it is sufficient to find a fixed grid which sums all $Y_{l''m}$ to zero, for $1\le l''\le l+l'$. McLaren[62] has discussed such grids in detail. The vertices of the regular tetrahedron, octahedron, and icosahedron with constant weighting factors provide grids of 4, 6, and 12 points which give exact integration of all functions with $l''\le 2$, 3, and 5, respectively. In cartesian coordinates, the four tetrahedral grid points are $(1/\sqrt{3},\ 1/\sqrt{3},\ 1/\sqrt{3})$, $(1/\sqrt{3},\ -1/\sqrt{3},\ -1/\sqrt{3})$, $(-1/\sqrt{3},\ 1/\sqrt{3},\ -1/\sqrt{3})$, and $(-1/\sqrt{3},\ -1/\sqrt{3},\ 1/\sqrt{3})$. The six octahedral grid points are $(\pm1,0,0)$, $(0,\pm1,0,0)$, and $(0,0\pm1)$. The 12 icosahedral points are $(0,\pm\lambda,\pm\rho)$, $(\pm\lambda,0,\pm\rho)$, and $(\pm\lambda,\pm\rho,0)$, where $\lambda=[(5-\sqrt{5})/10]^{1/2}$ and $\rho=[(5+\sqrt{5})/10]^{1/2}$. For applications in carbon and silicon, we have found the tetrahedral grid to be sufficient.

APPENDIX D: OPTIMAL AMOUNT OF SAMPLING OF THE NONLOCAL POTENTIAL

Let us suppose that we take M "samples" of the nonlocal potential at each step of the walk. For instance, if we are using the four-point grid which is exact for the s projection operator acting on s, p, and d wave functions, as described in Appendix C, by one "sample," we mean one randomly chosen four-point grid. The variance associated with the statistical evaluation of the nonlocal pseudopotential (as opposed to its exact evaluation at each point of the walk) will then be $\sigma_{\text{nonloc}}^2/M$, where σ_{nonloc} is the standard deviation of one four-point grid estimate of the nonlocal energy. [We should emphasize at this point that there is a variance in the nonlocal energy along the random walk even when the integral in Eq. (46) is evaluated exactly at each point. This variance is due to the variation of the nonlocal potential within the unit cell of the crystal. It is intrinsic to the problem and is quite separate from the variance due to statistical evaluation of the integral in Eq. (46).]

If T_{nonloc} is the computation time spent taking one "sample," the time spent sampling the nonlocal potential at each step of the random walk will be MT_{nonloc}. Let us denote the computation time spent doing all other work for each step in the random walk by T_{other} and define the quantity $x=T_{\text{other}}/T_{\text{nonloc}}$. Then the total time for an n-point walk is proportional to $(x+M)n$.

If we assume that the statistical variations due to sampling the nonlocal potential (instead of exact evaluation of the spherical integral) are independent of the statistical variations in the exact single-particle energy along the walk,[63] then

$$\sigma_{\text{tot}}^2=\frac{1}{n}(\sigma_{\text{exact}}^2+\sigma_{\text{nonloc}}^2/M)\ , \tag{D1}$$

where σ_{tot} is the combined standard deviation in the n-point walk average of the single-particle energy due to *all* variations, and σ_{exact} is the standard deviation of the exact single-particle energy along the walk.

For *optimal sampling* we want to minimize the total variance of an n-point walk average subject to the constraint that the total computation time is kept constant; i.e., $(x+M)n=t$ is constant. Writing n in terms of x, M, and t, we have

$$\sigma_{\rm tot}^2=\frac{(x+M)}{t}(\sigma_{\rm exact}^2+\sigma_{\rm nonloc}^2/M)\ . \tag{D2}$$

Setting the partial derivative with respect to M equal to zero, we find that the optimal value of M is achieved when

$$\frac{x}{M}=\frac{\sigma_{\rm exact}^2}{\sigma_{\rm nonloc}^2/M}\ . \tag{D3}$$

So the best strategy is to have the ratio of time spent doing other work to time spent sampling the nonlocal potential equal to the ratio of the variance of the exact energy to the nonlocal sampling variance.

[1]W. L. McMillan, Phys. Rev. **138**, A442 (1965).

[2]D. Ceperley, G. V. Chester, and M. H. Kalos, Phys. Rev. B **16**, 3081 (1977).

[3]D. M. Ceperley and B. J. Alder, Phys. Rev. Lett. **45**, 566 (1980).

[4]P. J. Reynolds, D. M. Ceperley, B. J. Alder, and W. A. Lester, J. Chem. Phys. **77**, 5593 (1982); R. M. Grimes, B. L. Hammond, P. J. Reynolds, and W. A. Lester, *ibid.* **85**, 4749 (1986).

[5]D. M. Ceperley and B. J. Alder, Phys. Rev. B **36**, 2092 (1987).

[6]The amount of computation time increases at least as $Z^{5.5}$; see D. M. Ceperley, J. Stat. Phys. **43**, 815 (1986).

[7]B. L. Hammond, P. J. Reynolds, and W. A. Lester, J. Chem. Phys. **87**, 1130 (1987).

[8]P. Hohenberg and W. Kohn, Phys. Rev. **136**, B864 (1964); W. Kohn and L. J. Sham, Phys. Rev. **140**, A1133 (1965).

[9]O. Gunnarsson and R. O. Jones, Phys. Rev. B **31**, 7588 (1985), and references therein.

[10]V. Heine, in *Solid State Physics*, edited by H. Ehrenreich, F. Seitz, and D. Turnbull (Academic, New York, 1970), Vol. 24, p. 24, and references therein.

[11]D. R. Hamann, M. Schlüter, and C. Chiang, Phys. Rev. Lett. **43**, 1494 (1979).

[12]P. A. Christiansen, Y. S. Lee, and K. S. Pitzer, J. Chem. Phys. **71**, 4445 (1979).

[13]C. M. Rohlfing and P. J. Hay, J. Chem. Phys. **83**, 4641 (1985).

[14]G. B. Bachelet, D. M. Ceperley, and M. G. B. Chiochetti, Phys. Rev. Lett. **62**, 2088 (1989).

[15]M. M. Hurley and P. A. Christiansen, J. Chem. Phys. **86**, 1069 (1987); P. A. Christiansen, *ibid.* **88**, 4867 (1988).

[16]T. Yoshida and K. Iguchi, J. Chem. Phys. **88**, 1032 (1988).

[17]B. L. Hammond, P. J. Reynolds, and W. A. Lester, Phys. Rev. Lett. **61**, 2312 (1988).

[18]A brief report of this method was given in S. Fahy, X. W. Wang, and S. G. Louie, Phys. Rev. Lett. **61**, 1631 (1988).

[19]L. Brewer, Lawerence Berkeley Laboratory Report No. LBL-3720 (unpublished).

[20]K. F. Zmbov, L. L. Ames, and J. L. Margrave, High Temp. Sci. **5**, 235 (1973).

[21]E. A. Gulbransen, K. F. Andrew, and F. A. Brassart, J. Electrochem. Soc. **113**, 834 (1966).

[22]S. G. Davis, D. F. Anthrop, and A. W. Searcy, J. Chem. Phys. **34**, 659 (1961).

[23]R. L. Batdorf and F. M. Smits, J. Appl. Phys. **30**, 259 (1959).

[24]P. Grieveson and L. B. Alcock, in *Special Ceramics*, edited by P. Popper (Academic, London, 1960).

[25]J. Drowat, G. De Maria, and M. G. Inghram, J. Chem. Phys. **29**, 1015 (1958).

[26]C. E. Moore, *Atomic Energy Levels* (U.S. GPO, Washington, D.C., 1949), Vol. 1.

[27]L. I. Schiff, *Quantum Mechanics*, 3rd ed. (McGraw-Hill, New York, 1968), p. 255.

[28]For a recent introduction to Monte Carlo methods, see K. Binder and D. W. Heermann, *Monte Carlo Simulation in Statistical Physics* (Springer, Berlin, 1988).

[29]N. Metropolis, A. W. Rosenbluth, M. N. Rosenbluth, A. H. Teller, and E. Teller, J. Chem. Phys. **21**, 1087 (1953).

[30]This is a consequence of the central-limit theorem of statistics.

[31]A. Bijl, Physica (Amsterdam) **7**, 869 (1940).

[32]N. F. Mott, Philos. Mag. **40**, 61 (1949).

[33]R. B. Dingle, Philos. Mag. **40**, 573 (1949).

[34]R. Jastrow, Phys. Rev. **98**, 1479 (1955).

[35]E. Feenberg, *Theory of Quantum Fluids* (Academic, New York, 1969).

[36]B. Kiel, G. Stollhoff, C. Weigel, P. Fulde, and H. Stoll, Z. Phys. B **46**, 1 (1982); G. Stollhoff and K. P. Bohnen, Phys. Rev. B **37**, 4678 (1988).

[37]E. Krotscheck and W. Kohn, Phys. Rev. Lett. **57**, 862 (1986); E. Krotscheck, Phys. Rev. B **31**, 4267 (1985); E. Krotscheck, W. Kohn, and G.-X. Qian, *ibid.* **32**, 5693 (1985).

[38]D. M. Ceperley and M. H. Kalos, in *Monte Carlo Methods in Statistical Physics*, 2nd ed., edited by K. Binder (Springer, Berlin, 1986).

[39]D. Ceperley, Phys. Rev. B **18**, 3126 (1978).

[40]D. Bohm and D. Pines, Phys. Rev. **92**, 609 (1953).

[41]H. Raether, *Excitation of Plasma and Interband Transitions by Electrons* (Springer, Berlin, 1980).

[42]F. Gygi and A. Baldereschi, Phys. Rev. B **34**, 4405 (1986).

[43]J. R. Chelikowsky and S. G. Louie, Phys. Rev. B **29**, 3470 (1984); C. T. Chan, D. Vanderbilt, and S. G. Louie, *ibid.* **33**, 2455 (1986).

[44]J. Ihm, A. Zunger, and M. L. Cohen, J. Phys. C **12**, 4409 (1979).

[45]J. M. Ziman, *Principles of the Theory of Solids*, 2nd ed. (Cambridge University Press, London, 1972), pp. 37–41.

[46]S. G. Louie, K. M. Ho, and M. L. Cohen, Phys. Rev. B **19**, 1774 (1979).

[47]M. S. Hybertsen and S. G. Louie, Phys. Rev. Lett. **55**, 1418 (1985); Phys. Rev. B **34**, 5390 (1986).

[48]P. P. Ewald, Ann. Phys. (Leipzig) [Folge 4] **64**, 253 (1921); B. R. A. Nijboer and F. W. deWette, Physica (Amsterdam) **23**, 309 (1957).

[49]D. G. Mahan, *Many-Particle Physics* (Plenum, New York, 1981), p. 374.

[50]G. D. Mahan, Ref. 49, p. 396.

[51]D. Ceperley (private communication).

[52]J. P. Perdew and A. Zunger, Phys. Rev. B **23**, 5048 (1981).

[53]F. D. Murnaghan, Proc. Nat. Acad. Sci. USA **3**, 244 (1944).

[54]J. Donohue, *The Structures of the Elements* (Krieger, Florida, 1982).

[55]H. J. McSkimin and P. Andreatch, Jr., J. Appl. Phys. **43**, 985 (1972).

[56]S. Fahy and S. G. Louie, Phys. Rev. B **36**, 3373 (1987); J. R.

Chelikowksky and S. G. Louie, *ibid.* **29**, 3470 (1984); G. B. Bachelet, H. S. Greenside, G. A. Baraff, and M. Schlüter, *ibid.* **24**, 4745 (1981); M. T. Yin and M. L. Cohen, *ibid.* **24**, 6121 (1981).

[57]For an analysis of this problem in graphite, see C. Pisani, R. Dovesi, and C. Roetti, *Hartree-Fock Ab Initio Treatment of Crystalline Systems* (Springer, Berlin, 1988).

[58]C. Kittel, *Introduction to Solid State Physics, 5th ed.* (Wiley, New York, 1976).

[59]B. Harmon, W. Weber, and D. R. Hamann, Phys. Rev. B **25**, 1109 (1982).

[60]M. V. Ganduglia-Pirovano, G. Stollhoff, P. Fulde, and K. P. Bohnen, Phys. Rev. B **39**, 5156 (1989).

[61]J. Phys. Chem. Ref. Data **14**, Suppl. 1, 1795 (1985).

[62]A. D. McLaren, J. Math. Comput. **17**, 361 (1963).

[63]This assumption is not rigorously justified. For instance, the statistical variation in the spherical integral tends to zero near the atoms, and so it cannot be completely uncorrelated with the variations in the exact energy. However, we expect the correlation to be weak and the conclusion of this appendix to be qualitatively correct.